Title
Identification of a cholesterol metabolic-type I interferon inflammatory circuit

Author
York, Autumn Gabrielle

Publication Date
2015

Peer reviewed|Thesis/dissertation

UNIVERSITY OF CALIFORNIA

Los Angeles

Identification of a cholesterol metabolic-type I interferon inflammatory circuit

A dissertation submitted in partial satisfaction of the

requirements for the degree Doctor of Philosophy

in Molecular and Medical Pharmacology

By

Autumn Gabrielle York

2015

ABSTRACT OF THE DISSERTATION

Identification of a cholesterol metabolic-type I interferon inflammatory circuit

By

Autumn Gabrielle York

Doctor of Philosophy in Molecular and Medical Pharmacology

University of California, Los Angeles, 2015

Professor Steven J. Bensinger, Chair

Cellular lipid requirements are achieved through a combination of biosynthesis and import programs. To date, the molecular mechanisms that regulate whether a cell preferentially scavenges or synthesizes lipids is not well understood, particularly in non-metabolic tissues, such as immune cells. Perturbations in fatty acid and cholesterol homeostasis have been observed in response to a number of viral and microbial infections, leading us to ask if signaling through immune receptors could influence the cellular programs that regulate lipid homeostasis in macrophage. Using mass spectrometry and isotope tracer analysis, we find that activation of Toll-like Receptors (TLRs) can broadly promote a lipid-scavenging program, however, only select TLRs can specifically limit *de novo* synthesis of both fatty acids and cholesterol. We find that TLR- and virus-mediated production of type I interferon is responsible for inhibition of flux through the lipid biosynthetic program, resulting in a shift in macrophage metabolism to favor

lipid import over synthesis. Genetically enforcing this metabolic shift in macrophages is sufficient to render mice resistant to viral challenge, demonstrating the importance of reprogramming the balance of these two metabolic pathways *in vivo*. Unexpectedly, mechanistic studies reveal that limiting flux through the cholesterol biosynthetic pathway spontaneously engages a type I IFN response in a STING-dependent manner. The upregulation of type I IFNs was traced to a decrease in the pool size of synthesized cholesterol, and replenishing cells with free cholesterol could inhibit STING-mediated production of type I IFNs. Taken together, these data support a model where perturbations in cholesterol biosynthetic flux intrinsically influence the STING signaling cascade and provide a molecular mechanism linking cholesterol homeostasis with type I IFN-mediated inflammation. In sum, these studies delineate a metabolic-inflammatory circuit that links perturbations in cholesterol biosynthesis with activation of innate immunity.

The dissertation for Autumn Gabrielle York is approved.

Heather R. Christofk

Caius G. Radu

Peter Tontonoz

Steven J. Bensinger, Committee Chair

University of California, Los Angeles

2015

DEDICATION

This thesis is dedicated to the two most influential women in my life, my mother Millie Carol York and my grandmother Janet Lewis Hardesty.

TABLE OF CONTENTS

TABLE OF CONTENTS

Continued

ACKNOWLEDGEMENTS

I would like to thank my mentor Dr. Steven Bensinger for his outstanding support and guidance over the past 5.5 years. I'm so thankful for the opportunities that I have been provided while in his lab.

I would like to thank my committee members Dr. Heather Christofk, Dr. Caius Radu and Dr. Peter Tontonoz for their support and guidance throughout graduate school.

I would like to acknowledge my coauthors Kevin J. Williams (UCLA), Joseph P. Argus (UCLA), Quan "Dylan" Zhou (UCLA), Gurpreet Brar (UCLA), Laurent Vergnes (UCLA), Elizabeth E. Gray (University of Washington, Seattle), Anjie Zhen (UCLA), Nicholas C. Wu (UCLA), Douglas H. Yamada (UCLA), Cameron R. Cunningham (UCLA), Elizabeth J. Tarling (UCLA), Moses Q. Wilks (UCLA), David Casero (UCLA), David H. Gray (UCLA), Amy K. Yu (UCLA), Eric S. Wang (UCLA), David G. Brooks (UCLA), Ren Sun (UCLA), Scott G. Kitchen (UCLA), Ting-Ting Wu (UCLA), Karen Reue (UCLA), and Daniel B. Stetson (University of Washington, Seattle) for their help with my manuscript "Limiting cholesterol biosynthetic flux engages type I interferon signaling in a STING-dependent manner". I would like to acknowledge Dr. Steven Smale and his lab members Dr. Ann-Jay Tong and Xin Liu for their help with the chromatin-associated transcripts studies and upcoming ChIP assays.

I would like to acknowledge Dylan Taatjes, Krista Meyer, Noah Dowell and Dominique Liserio. I would not be the scientist I am today without each of you.

My research was supported in part by California HIV/AIDS Research Program Training Fellowship (D12-LA-351) and UCLA Dissertation Year Fellowship.

VITA

EDUCATION:

B.A. in Biochemistry (*Magna Cum Laude*) and B.A. in Molecular, Cellular & Developmental Biology, (with a Chemistry Minor), University of Colorado, Boulder, CO; May 2008

PUBLICATIONS:

1. **Autumn G. York**, Kevin J. Williams, Joseph P. Argus, Quan D. Zhou, Gurpreet Brar1, Laurent Vergnes, Elizabeth E. Gray, Anjie Zhen, Nicholas C. Wu, Douglas H. Yamada, Cameron R. Cunningham, Elizabeth J. Tarling, Moses Q. Wilks, David Casero, David H. Gray, Amy K. Yu, Eric S. Wang, David G. Brooks, Ren Sun, Scott G. Kitchen, Ting-Ting Wu, Karen Reue, Daniel B. Stetson and Steven J. Bensinger (2015) *Limiting Cholesterol Biosynthetic Flux Spontaneously Engages Type I IFN Signaling.* Cell. December 17th. Vol. 163, Issue 7. p1716-1729
2. **Autumn G. York** and Steven J. Bensinger (2013) *Subverting sterols: rerouting an oxysterol-signaling pathway to promote tumor growth.* Journal of Experimental Medicine. August. Vol. 210 no. 9 p1653-1656
3. Ethan Ahler, William Juster Sullivan, Ashley Cass, Daniel Braas, **Autumn G. York**, Steven Bensinger, Thomas Graeber, and Heather Christofk (2013) *Doxycycline alters metabolism and proliferation of human cell lines.* PLoS ONE 8(5): e64561. doi:10.1371/journal.pone.0064561
4. Kevin Williams, Joseph Argus, Yue Zhu, Moses Wilks, Beth Marbois, **Autumn G. York**, Yoko Kidani, Alexandra Pourzia, David Akhavan, Dominique Lisiero, Evangelia Komisopoulou, Amy Henkin, Horacio Soto, Brian Chamberlain, Laurent Vergnes, Michael Jung, Jorge Torres, Linda Liau, Heather Christofk, Robert Prins, Paul Mischel, Karen Reue, Thomas Graeber, and Steven Bensinger (2013). *An essential requirement for the SCAP/SREBP signaling axis to protect cancer cells from lipotoxicity*. Cancer Research. May 1;73(9):2850-62
5. Yongxin Yu, Chunying Song, Oiongyi Zhang, Peter DiMaggio, Benjamin Garcia, **Autumn York**, Michael Carey, Michael Grunstein (2012) *Histone H3 Lysine 56 Methylation Regulates DNA Replication through Its Interaction with PCNA.* Molecular Cell. April 13;46 (1):7-17
6. Krista Meyer, Aaron Donner, Matthew Knuesel**, Autumn G. York**, Joaquin Espinosa, Dylan Taatjes (2008) *Cooperative activity of cdk8 and GCN5L within Mediator directs tandem phosphoacetylation of histone H3*. The EMBO Journal. Vol 27 (10) p1449

AWARDS & HONORS:

1. Best Poster Award. UCLA Molecular and Medical Pharmacology Retreat. October 2015
2. The American Association of Immunology Young Investigator Award at ImmunologyLA 2015. Los Angeles, CA. May 2015.
3. Trainee Poster Award. American Association of Immunologists Annual Conference: IMMUNOLOGY 2015. New Orleans, LA. May 2015
4. Trainee Abstract Award. American Association of Immunologists Annual Conference: IMMUNOLOGY 2014. Abstract selected for short talk. May 2014. Pittsburgh, PA

5. Best Student Talk at Department of Molecular and Medical Pharmacology Student Seminar Series. UCLA. 2012-2013.
6. Graduate Division Dissertation Year Fellowship. Department of Molecular and Medical Pharmacology. UCLA. January. 2014-2015
7. California HIV/AIDS Research Program Pre-Doctoral Training Fellowship. March 2013-March 2015
8. Abstract selected for short talk. American Society for Molecular Biology and Biochemistry, Section Title: Lipids and Infection. Oral Presentation Title "*Defining the Role of SREBPs in Hepatitis C Viral Infection"* April 2012; San Diego, CA
9. Student Travel Award. Molecular and Medical Pharmacology. UCLA. April 2012
10. *In Vivo* Cell and Molecular Imaging Center Career Development Training Award. UCLA Dec 2010
11. *Magna Cum Laude* graduation honors. University of Colorado-Boulder, Department of Biochemistry, Thesis Title: *Structural and Functional Examination of Sp1/SREBP-Mediator Transcriptional Synergy*. May 2008
12. Chris Severy Outstanding Undergraduate Research Award, University of Colorado-Boulder, Department of Chemistry & Biochemistry, 2008
13. Outstanding Poster Award, University of Colorado-Boulder, Department of Chemistry & Biochemistry Undergraduate Research Symposium, 2007, 2008
14. HHMI/UROP Bioscience Fellowship; University of Colorado. 2005-2006, 2006-2007, 2007-2008
15. Biological Sciences Initiative Undergraduate Travel Award. University of Colorado 2007, 2008
16. Summer Undergraduate Research Fellowship. University of Colorado-Boulder 2007

PRESENTATIONS:

1. UCLA Molecular and Medical Pharmacology Retreat. Poster Title: *"Reprogramming lipid metabolism primes host antiviral immunity"*. October 2015. Huntington Beach, CA
2. ImmunologyLA. Oral Presentation. Talk title: Limiting cholesterol biosynthetic flux engages antiviral immunity. Los Angeles, CA May 2015.
3. American Association of Immunologists Annual Conference: IMMUNOLOGY 2015. Poster Title: "*Reprogramming lipid metabolism primes host antiviral immunity*". May 2015. New Orleans, LA
4. UCLA Molecular and Medical Pharmacology Retreat. Oral Presentation. Title: *"Reprogramming lipid metabolism primes host antiviral immunity"*. November 2014. Huntington Beach, CA
5. American Association of Immunologists Annual Conference: IMMUNOLOGY 2014. Oral Presentation. Talk Title: "*Reprogramming lipid metabolism primes host antiviral immunity*". May 2014. Pittsburgh, PA
6. The 19th International Symposium on Hepatitis C Virus and Related Viruses. Poster Title: "*Inhibition of SREBP Processing hinders HCV Infection*". October 2012; Venice, Italy.
7. UCLA Molecular and Medical Pharmacology Retreat. Oral Presentation. Title: *"Defining the Role of SREBPs in HCV infection"*. November 2012. Huntington Beach, CA
8. American Society of Biochemistry and Molecular Biology Conference: Lipids and Infection. Oral Presentation: "*Defining the Role of SREBPs in Hepatitis C Viral Infection"* April 2012; San Diego, CA
9. UCLA Molecular and Medical Pharmacology Retreat. Poster. October 2010 & 2011. Huntington Beach, CA.

CHAPTER 1:

An introduction to macrophage biology and lipid metabolism

A brief introduction to macrophage biology and innate immunity

Macrophages (derived from Greek for “big eaters”) are specialized innate immune cells that play vital roles in host defense, wound healing and phagocytosis [1]. Macrophages can be derived from the myeloid lineage of the hematopoietic stem cell niche in the bone marrow [2,3]. Monocytes, a precursor to bone marrow-derived macrophages, circulate in the blood until they are recruited to areas of infection where they differentiate into macrophage [3]. Conversely, tissue-resident macrophages are a long-lived population of macrophages that are present in most tissues of the body the absence of infection [4,5]. These subpopulations of macrophages originate from yolk-sac-dervived erythro-meyloid progenitors and are maintained through self-renewal or monocyte recruitment, depending on the tissue location [4]. Tissue-resident macrophages show a great heterogeneity between subpopulations, indicative of specialized functions acquired within various tissue niches [5]. In this context, tissue-resident macrophages provide surveillance for foreign substances in these tissues and are the first line of defense against invading pathogens. Macrophages are equipped with an array of Toll-like Receptors (TLRs), capable of broadly identifying an array of pathogens via pathogen-associated molecular patterns (PAMPs) [6]. In this way, macrophages generate an innate immune response that generically identifies classes of pathogens (virus, bacteria, fungus, parasite). While TLR stimulation engages specific gene programs to promote clearance of recognized class of pathogen, recruitment of the adaptive immune system is required mount an antigen-specific immune response [6]. Indeed, signaling though macrophage TLRs initiates the production of cytokines and chemokines, soluble molecules that recruit additional monocyte-derived macrophages and other cells of the adaptive immune system to the area of infection [2]. In addition to pathogen clearance, macrophage can also clear dead cells and debris found within tissue.

Perhaps the best-defined example of the crosstalk between lipids and innate immunity has been described in the pathogenesis of atherosclerosis and related cardiovascular diseases. A hallmark of atherosclerosis is fatty depositions, in particular cholesterol and triglycerides, in the arterial wall (reviewed in [7,8]). This is accompanied by infiltrating mononuclear cells and the generation of robust pro-inflammatory responses by lipid loaded macrophage dubbed foam cells [9].

A primer on lipid composition

Lipids are a naturally occurring group of molecules that play key biological roles in membrane structure, energetics and signaling. Types of lipids include sterols, fatty acids (mono-, di-, triglycerides and phospholipids), eicosanoids (ie prostaglandins, leukotirenes, etc), oxysterols, fat-soluble vitamins and others. The majority of cellular lipids are found within cellular membranes, representing approximately 40% of total cellular mass. Lipid composition of membranes directly regulates the function of cells through their ability to influence biochemical processes (e.g., signaling) and biophysical properties (e.g., membrane permeability or fluidity) [10]. The lipid composition of cellular membranes is highly heterogeneous, composed of many classes of glycerophospholipids and sterols. Additionally, membranes are heterotypic, meaning that inner and outer leaflets of membranes are distinct from each other in their lipid composition [11]. Finally, the lipid composition of cellular membranes can be distinct depending on cell type (e.g., erythrocyte versus lymphocyte) or cellular state (quiescent versus activated).

Cholesterol homeostasis

In immune cells, nearly all cholesterol is found within plasma and organelle membranes; however there may be small pools of esterified cholesterol (cholesterol linked to a long chain fatty acid) that serve to store excess cholesterol within the cytosol. Cholesterol is exceedingly hydrophobic and must be shuttled between intracellular compartments through the activity of

Niemann-Pick type proteins and other protein transporters (e.g., Star proteins) [12]. In the absence of these proteins, sterols aberrantly accumulate in membranes, resulting in severe cellular dysfunction and apoptosis. While it might seem intuitive that cholesterol would be equally distributed throughout the entirety of a cell's membrane bilayers (e.g., plasma, endoplasmic reticulum (ER) and glogi membranes), in fact there is considerable difference in the cholesterol content between organelle and plasma membranes within a given cell [13]. Elegant subcellular fractionation studies revealed that under steady state conditions, the amount of cholesterol residing in the plasma membrane is approximately 10X greater than the amount found in the ER membrane from the same cells. As to how this gradient in cholesterol levels between subcellular compartments maintained remains very poorly understood. Nevertheless, this difference appears to be critically important for regulation of cholesterol content. Nearly all of the "sterol" sensing proteins involved in cholesterol homeostasis are embedded in the ER, and are exquisitely sensitive to changes in pool sizes of ER cholesterol [14]. It has been estimated that exceedingly small changes in ER membrane cholesterol, on the order of 1-2 % change on a molar basis is sufficient to induce functional changes in the sterol sensing apparatus and regulation of the cholesterol biosynthetic program [13]. This exceptionally tight regulation in ER cholesterol content is consistent with the idea that different intracellular cholesterol pools can be monitored independently, and may convey different physiologic signals to a cell [15].

Fatty acid homeostasis

The majority of cellular fatty acids (FAs) are long (14-20 carbons) and very chain hydrocarbons (22-26 carbons) [11]. These FA molecules are generally incorporated into more complex lipids, such as phospholipids, sphingomyelins, triacylglycerides (TG), and glycolipids. These complex lipids predominately contribute to plasma and organelle membranes biomass, but can also serve as neutral lipid storage for energy (e.g., TG), signaling molecules (PA, DAG, etc), and

protein modifications (e.g., palmitoylation). FAs also vary in their degree of desaturation (i.e., numbers of double bonds). Saturated FAs have no double bonds (termed SFAs), monounsaturated FAs (MUFAs) have a single double bond, and poly unsaturated FAs (PUFAs) have more than two double bonds. Most long chain FAs can either be synthesized as long chain hydrocarbons and then chemically modified through a series of enzymes (e.g., elongation or desaturated), or scavenged from the environment, before use or modification as required (e.g., elongated or desaturated). However, there are some FAs that mammalian cells are unable to make, and are deemed essential because they must come from must be dietary sources (e.g., linoleic acid 18:2). The intrinsic complexity in defining the sources of cellular lipids, and the flux of lipids from one pool to another lipid pool (e.g., saturated to desaturated) poses a significant technical and scientific barrier to defining how lipid composition is remapped in response to activation or cytokine signals. In our laboratory, we have developed isotope-labeling techniques and mathematical modeling approaches (termed metabolic flux analysis [16]) that allow us to address these important biologic processes in primary immune cells. This technique was applied to the studies in chapter 2 of this dissertation, where we examine how activation or cytokine signals dynamically change the lipid composition of primary macrophages.

Cellular lipids pools may not be functionally interchangeable

Cellular cholesterol and fatty acid requirements can be met by either: 1) scavenging from environmental sources via receptor-mediated endocytosis, or 2) *de novo* synthesis from the Acetyl-CoA metabolite pool via a complex series of enzymatic reactions in the ER (Voet and Voet, 2011). All cells have the ability to perform both of these processes. To date, the molecular mechanisms that regulate whether a cell preferentially scavenges or synthesizes cholesterol or fatty acids is not well understood, particularly in non-metabolic tissues, such as immune cells. Nor is it clear if fatty acids or cholesterol derived from a scavenged source or a synthesized pool are functionally interchangeable. Indeed, our group recently published that biosynthesis of

cholesterol is required for efficient cell cycle progression and acquisition of effector cell function in response to TCR signals in primary T cells [17]. Mechanistic studies demonstrated that *de novo* synthesis of cholesterol conveys a "fitness" signal to newly activated CD8 T cells, resulting in the ability of a cell to add substantial ER membrane during G1 of cell cycle. Likewise, recent studies on CD8 T cells indicates that memory T cells use a previously poorly defined futile cycle where they synthesize fatty acids and TGs but immediately burn them for energetics [18]. As to why the cells would not scavenge FAs has not been elucidated, but it is clear that this cycle is critical for survival and function of memory CD8 T cells. In combination, these studies have led us to posit that scavenged and synthesized pools of lipids are not necessarily functionally interchangeable.

An introduction to the transcriptional regulation of lipid homeostasis

Three families of transcription factors are responsible for maintenance of lipid homeostasis: Sterol Regulatory Element Binding Proteins (SREBPs), Liver X Receptors (LXRs) and Peroxisome Proliferator-Activator Receptors (PPARs). While each family of transcription factors regulates a diverse set of lipid metabolism genes, together these transcription factor families support integrated and dynamic programs to maintain lipid homeostasis in response to various external stimuli.

SREBPs: SREBPs are the master transcriptional regulators of cholesterol and fatty acid biosynthesis, trans-activating nearly all genes required for de novo cholesterol and fatty acid biosynthesis. In addition to activation lipid biosynthesis, SREBPs also regulate lipid import via transcriptional regulation of the low density lipoprotein receptor (LDLR) [19]. In mammals there are two SREBP genes that express three SREBP proteins (SREBF1 and SREBf2). SREBP1a and SREBP1c are produced via alternative transcriptional start sites on *SREBF1*, whereas the *SREBF2* gene encodes SREBP2. SREBP1c activates transcription of genes involved in fatty

acid synthesis, while SREBP2 is responsible for transcriptionally activating genes required for cholesterol synthesis. SREBP1a is capable of transcriptionally activating both SREBP1c and SREBP2 target genes [19].

SREBPS are subject to complex regulation. Full length SREBPs are embedded in the endoplasmic reticulum (ER) membrane, in close association with the sterol-sensing domain-containing proteins SCAP (SREBP Cleavage Activating Protein) and INSIGs (Insulin Induced Gene 1 and 2) [14]. When ER sterol levels are low, SREBP/SCAP heterodimers are released from INSIG and are shuttled to the golgi via COPII vesicle transport. Two proteases in the golgi, site 1 and site 2 proteases sequentially cleave SREBPs liberating the N-terminal domain of SREBP. This process exposes a nuclear localization sequence, allowing the cleaved mature form of SREBP to enter the nucleus and bind to Sterol Response Elements (SREs) to initiate transcription (see Figure 1 for model). Addition of exogenous cholesterol is capable of repressing SREBP maturation and transcriptional activity by preventing SCAP/SREBP ER-to-golgi transport. Furthermore, active SREBPs are negatively regulated in the nucleus through posttranslational modification including deacetylation by sirtuins and ubiquitination by E3 ligase FBW7 resulting in clearance by the 26S proteasome [20,21].

LXRs: LXRs are members of the nuclear receptor superfamily of transcription factors. There are two isoforms of LXR, alpha and beta (NR1H3 and NR1H1), both of which require ligand binding for transcriptional activation. LXR isoforms form obligate heterodimers with retinoid X receptor (RXR). LXR-alpha is expressed highly in the liver and to a lesser extent in adipose tissue, spleen, kidney, intestine and macrophage, while LXRβ expression is maintained in most tissues types. The natural ligands of LXRs are oxidized derivatives of cholesterol, known as oxysterols, and the intermediary metabolites of cholesterol biosynthetic pathway (such as desmosterol) [22-24]. In the absence of ligand, most LXR/RXR heterodimers are bound to DNA in association

with co-repressors and chromatin modifying complexes that enforce target gene repression. Upon activation, LXRs regulate a gene program that can effectively remove cellular cholesterol through efflux pathways (also called reverse cholesterol transport) [25]. Additionally, LXRs inhibit cholesterol import via transcriptional regulation of IDOL, an E3 ubiquitin ligase responsible for proteasome-mediated degradation of LDLR [26].

The well-defined role of LXRs in cholesterol efflux pathways has made this family of transcription factors particularly interesting in the context of atherosclerosis, where macrophage become lipid-laden and form plaques on arterial walls. Indeed, pharmacological activation of LXR improves limits atherosclerotic legion formation in mice pre-disposed to athersclerosis, whereas mice deficient in LXRs show enhanced atherosclerotic disease progression[27,28]. Additionally, LXRs have a clear role in limiting lipid-driven metabolic inflammation through their ability to trans-repress Nuclear Factor Kappa B (NFKB) activation downstream of TLR signaling. [7,9,22,23].

In the context of cellular cholesterol metabolism, LXRs play reciprocal roles to SREBPs (Figure 2). For example, when cellular sterol levels are low, SREBPs are shuttle to the golgi for activation. Activated SREBPs subsequently upregulated the enzymes required to *de novo* synthesize cholesterol, as well as LDLR to promote cholesterol uptake[19]. The intermediary metabolites of cholesterol biosynthesis activate LXR [22], which subsequently upregulates cholesterol efflux via ABCA1 and ABCG1 reverse-cholesterol transporters Additionally, LXR target gene IDOL promotes degradation of LDLR. In this system, the regulation of each pathway ensures that one pathway can sense changes in the other. This type of feed back mechanism maintains cholesterol homeostasis and safeguards against too much or too little cellular cholesterol (See Figure 2 for schematic).

PPARs: PPARs are also members of the nuclear receptor superfamily of transcription factors that form obligate heterodimers with RXR. The PPAR subfamily includes three proteins: PPAR-alpha, PPARbeta/delta and PPAR-gamma (NR1C1, NR1C2, and NR1C3), each with varying tissue expression levels [1,27]. Despite different tissue distribution, the PPAR family members have distinct, but overlapping biological functions. The ligands for PPARs are believed to be polyunsaturated fatty acids and eicosanoids, but the specific types of these molecules that regulate PPAR *in vivo* remain ambiguous [29] [1,27]. PPAR-alpha regulates fatty acid oxidation primarily in the liver, heart and brown fat [30]. PPARbeta/delta is expressed an all tissues of the body, and PPARbeta/delta target genes are broadly involved in fatty-acid metabolism, thermogenesis and mitochondrial respiration [1]. Finally, PPAR-gamma is expressed primarily in white adipose tissue and is critical for adipocyte differentiation [31]. While the biological roles and expression pattern vary between the PPAR isoforms, each PPAR isoform can upregulate reverse cholesterol transport (efflux) via ABCA1, a canonical LXR target gene. In line with this, specific agonists to each PPAR isoform can reduce atherosclerotic legion formation in mice predisposed to the disease[27,32,33]. Similar to LXR, PPARs are able to functionally repress inflammation through negative regulation of NFKB and other immune signaling cascades (Reviewed in [34,35]). However, the direct mechanism behind PPAR-mediation repression of inflammation is unknown.

Chapter 1: Figure 1

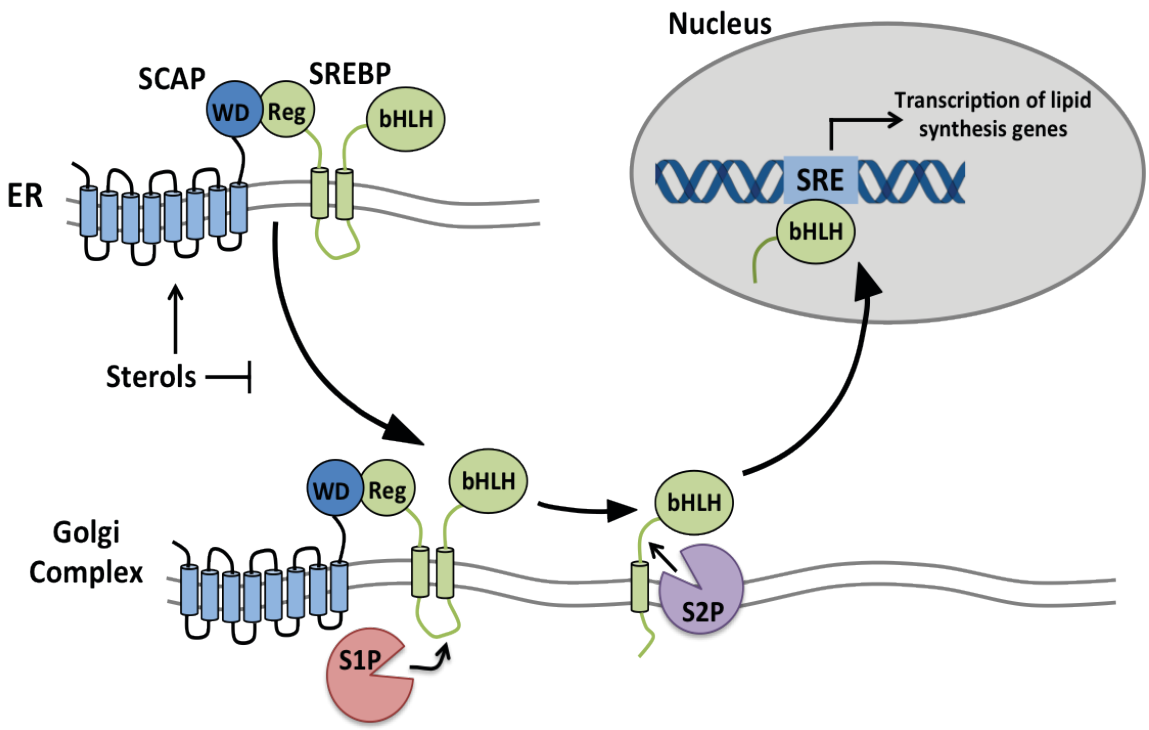

Chapter 1: Figure 1: SREBPS are subject to complex regulation. Full length SREBPs are embedded in the endoplasmic reticulum (ER) membrane, in close association with the sterol-sensing domain-containing proteins SCAP (SREBP Cleavage Activating Protein) and INSIGs (Insulin Induced Gene 1 and 2) (Goldstein et al., 2006). When ER sterol levels are low, SREBP/SCAP heterodimers are released from INSIG and are shuttled to the golgi via COPII vesicle transport. Two proteases in the golgi, site 1 and site 2 proteases sequentially cleave SREBPs liberating the N-terminal domain of SREBP. This process exposes a nuclear localization sequence, allowing the cleaved mature form of SREBP to enter the nucleus and bind to Sterol Response Elements (SREs) to initiate transcription. Addition of exogenous cholesterol is capable of repressing SREBP maturation and transcriptional activity by preventing SCAP/SREBP ER-to-golgi transport. Furthermore, active SREBPs are negatively regulated in the nucleus through posttranslational modification including deacetylation by sirtuins and ubiquitination by E3 ligase FBW7 resulting in clearance by the 26S proteasome (Sundqvist et al., 2005; Walker et al., 2010).

Chapter 1: Figure 2

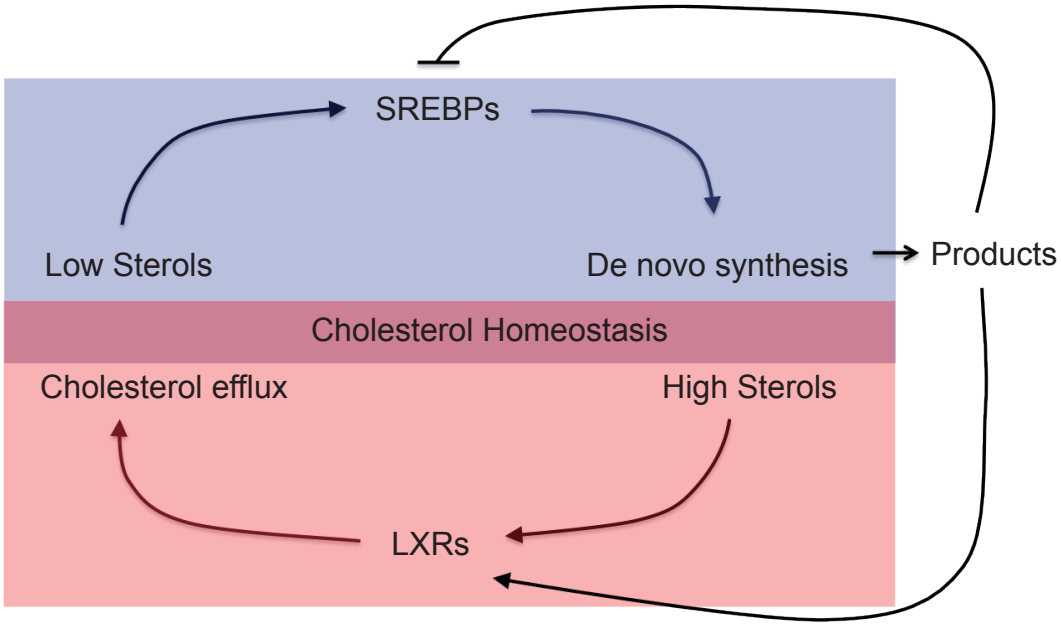

Chapter 1: Figure 2: SREBPS and LXRs have reciprocal actions in cholesterol metabolism. When cellular sterol levels are low, SREBPs are shuttle to the golgi for activation. Activated SREBPs subsequently upregulated the enzymes required to de novo synthesize cholesterol, as well as LDLR to promote cholesterol uptake. The intermediary metabolites of cholesterol biosynthesis activate LXR, which subsequently upregulates cholesterol efflux via ABCA1 and ABCG1 reverse-cholesterol transporters Additionally, LXR target gene IDOL promotes degradation of LDLR. In this system, the regulation of each pathway ensures that one pathway can sense changes in the other.

References for Chapter 1:

1. Bensinger SJ, Tontonoz P (2008) Integration of metabolism and inflammation by lipid-activated nuclear receptors. Nature 454: 470-477.

2. Murphy K, Travers P, Walport M, Janeway C (2008) Janeway's immunobiology. New York: Garland Science. xxi, 887 p. p.

3. Murray PJ, Wynn TA (2011) Protective and pathogenic functions of macrophage subsets. Nat Rev Immunol 11: 723-737.

4. Gomez Perdiguero E, Klapproth K, Schulz C, Busch K, Azzoni E, et al. (2015) Tissue-resident macrophages originate from yolk-sac-derived erythro-myeloid progenitors. Nature 518: 547-551.

5. Davies LC, Jenkins SJ, Allen JE, Taylor PR (2013) Tissue-resident macrophages. Nat Immunol 14: 986-995.

6. Janeway CA, Jr., Medzhitov R (2002) Innate immune recognition. Annu Rev Immunol 20: 197-216.

7. Glass CK, Witztum JL (2001) Atherosclerosis. the road ahead. Cell 104: 503-516.

8. Weber C, Noels H (2011) Atherosclerosis: current pathogenesis and therapeutic options. Nat Med 17: 1410-1422.

9. Shibata N, Glass CK (2009) Regulation of macrophage function in inflammation and atherosclerosis. J Lipid Res 50 Suppl: S277-281.

10. Voet D, Voet JG (2011) Biochemistry. Hoboken, NJ: John Wiley & Sons. xxv, 1428, 1453 p.

11. Vance DE, Vance JE (2008) Biochemistry of lipids, lipoproteins and membranes. Amsterdam ; Boston: Elsevier. xii, 631 p., 638 p. of plates p.

12. Wang ML, Motamed M, Infante RE, Abi-Mosleh L, Kwon HJ, et al. (2010) Identification of surface residues on Niemann-Pick C2 essential for hydrophobic handoff of cholesterol to NPC1 in lysosomes. Cell Metab 12: 166-173.

13. Radhakrishnan A, Goldstein JL, McDonald JG, Brown MS (2008) Switch-like control of SREBP-2 transport triggered by small changes in ER cholesterol: a delicate balance. Cell Metab 8: 512-521.

14. Goldstein JL, DeBose-Boyd RA, Brown MS (2006) Protein sensors for membrane sterols. Cell 124: 35-46.

15. Das A, Brown MS, Anderson DD, Goldstein JL, Radhakrishnan A (2014) Three pools of plasma membrane cholesterol and their relation to cholesterol homeostasis. Elife 3.

16. Williams KJ, Argus JP, Zhu Y, Wilks MQ, Marbois BN, et al. (2013) An essential requirement for the SCAP/SREBP signaling axis to protect cancer cells from lipotoxicity. Cancer Res 73: 2850-2862.

17. Kidani Y, Elsaesser H, Hock MB, Vergnes L, Williams KJ, et al. (2013) Sterol regulatory element-binding proteins are essential for the metabolic programming of effector T cells and adaptive immunity. Nat Immunol 14: 489-499.

18. Chang CH, Curtis JD, Maggi LB, Jr., Faubert B, Villarino AV, et al. (2013) Posttranscriptional control of T cell effector function by aerobic glycolysis. Cell 153: 1239-1251.

19. Horton JD, Goldstein JL, Brown MS (2002) SREBPs: activators of the complete program of cholesterol and fatty acid synthesis in the liver. J Clin Invest 109: 1125-1131.

20. Sundqvist A, Bengoechea-Alonso MT, Ye X, Lukiyanchuk V, Jin J, et al. (2005) Control of lipid metabolism by phosphorylation-dependent degradation of the SREBP family of transcription factors by SCF(Fbw7). Cell Metab 1: 379-391.

21. Walker AK, Yang F, Jiang K, Ji JY, Watts JL, et al. (2010) Conserved role of SIRT1 orthologs in fasting-dependent inhibition of the lipid/cholesterol regulator SREBP. Genes Dev 24: 1403-1417.

22. Spann NJ, Garmire LX, McDonald JG, Myers DS, Milne SB, et al. (2012) Regulated accumulation of desmosterol integrates macrophage lipid metabolism and inflammatory responses. Cell 151: 138-152.

23. Yang C, McDonald JG, Patel A, Zhang Y, Umetani M, et al. (2006) Sterol intermediates from cholesterol biosynthetic pathway as liver X receptor ligands. J Biol Chem 281: 27816-27826.

24. Traversari C, Sozzani S, Steffensen KR, Russo V (2014) LXR-dependent and -independent effects of oxysterols on immunity and tumor growth. Eur J Immunol 44: 1896-1903.

25. Venkateswaran A, Laffitte BA, Joseph SB, Mak PA, Wilpitz DC, et al. (2000) Control of cellular cholesterol efflux by the nuclear oxysterol receptor LXR alpha. Proc Natl Acad Sci U S A 97: 12097-12102.

26. Zelcer N, Hong C, Boyadjian R, Tontonoz P (2009) LXR regulates cholesterol uptake through Idol-dependent ubiquitination of the LDL receptor. Science 325: 100-104.

27. Castrillo A, Tontonoz P (2004) Nuclear receptors in macrophage biology: at the crossroads of lipid metabolism and inflammation. Annu Rev Cell Dev Biol 20: 455-480.

28. Lee SD, Tontonoz P (2015) Liver X receptors at the intersection of lipid metabolism and atherogenesis. Atherosclerosis 242: 29-36.

29. Giguere V (1999) Orphan nuclear receptors: from gene to function. Endocr Rev 20: 689-725.

30. Dreyer C, Keller H, Mahfoudi A, Laudet V, Krey G, et al. (1993) Positive regulation of the peroxisomal beta-oxidation pathway by fatty acids through activation of peroxisome proliferator-activated receptors (PPAR). Biol Cell 77: 67-76.

31. Tontonoz P, Hu E, Spiegelman BM (1994) Stimulation of adipogenesis in fibroblasts by PPAR gamma 2, a lipid-activated transcription factor. Cell 79: 1147-1156.

32. Graham TL, Mookherjee C, Suckling KE, Palmer CN, Patel L (2005) The PPARdelta agonist GW0742X reduces atherosclerosis in LDLR(-/-) mice. Atherosclerosis 181: 29-37.

33. Chawla A, Boisvert WA, Lee CH, Laffitte BA, Barak Y, et al. (2001) A PPAR gamma-LXR-ABCA1 pathway in macrophages is involved in cholesterol efflux and atherogenesis. Mol Cell 7: 161-171.

34. Klappacher GW, Glass CK (2002) Roles of peroxisome proliferator-activated receptor gamma in lipid homeostasis and inflammatory responses of macrophages. Curr Opin Lipidol 13: 305-312.

35. Straus DS, Glass CK (2007) Anti-inflammatory actions of PPAR ligands: new insights on cellular and molecular mechanisms. Trends Immunol 28: 551-558.

CHAPTER 2:

Toll-like Receptors selectively reprogram lipid metabolism

Introduction

Evidence indicates an intimate relationship exists between host lipid metabolism and intracellular pathogens [36-39]. Perturbations in host lipid homeostasis are observed in viral and microbial infections [40-42]. While it remains mechanistically unclear as to how each invading pathogen subverts host lipid metabolism, it has been proposed that co-opting of host metabolism is a general strategy employed by pathogens to meet the anabolic requirements of pathogen lifecycle, and facilitate evasion from host defense [40-45]. Consistent with this concept, genetic or pharmacologic inhibition of host lipid metabolism has been shown to attenuate pathogenesis of both viral and microbial infections in a number of model systems [42,46-51].

Cumulatively, these studies suggest that co-opting of host lipid metabolism facilitates microbial or viral pathogenesis, and leads to the hypothesis that host defense pathways should attempt to overwrite the metabolic changes induced by invading pathogens. In this way, the purpose of metabolic reprogramming observed in response to pro-inflammatory signals would be to create an unfavorable intracellular lipid metabolic environment. In support of this concept, recent studies have demonstrated that components of host responses to pathogens (e.g., TLR3/4 signaling, type I interferon and type II IFN signaling) specifically rewire components of the lipid metabolic program by downregulating *de novo* cholesterol biosynthesis at the genetic level [52-55]. Thus, it has been suggested that the influence of IFN signaling on the cholesterol homeostasis would serve to limit the availability of lipid metabolites for intracellular organisms. In contrast, other studies have shown that these same inflammatory signals (e.g., TLR3/4 signaling and type I IFNs) increase lipid uptake from environmental sources, resulting in the accumulation of neutral lipids, lipid droplets and ultimately facilitating foam cell formation (lipid loaded macrophages) [56-59]. Thus, it remains unclear if the purpose of type I IFN-mediated metabolic reprogramming is to specifically limit the availability of lipid metabolites (e.g.,

cholesterol) for pathogens as been proposed, or if there are alternative reasons for the selective reprogramming of flux through the cholesterol biosynthetic pathway.

Macrophages are critical moderators of the innate immune system and lipid metabolism [27]. While a number of studies indicate that macrophage activation can influence lipid homeostasis [22,60,61], the contribution of lipid scavenging versus lipid synthesis has yet to be evaluated in these cells. In this study, we find that activation of TLRs can broadly promote a lipid-scavenging program, however, only select TLRs can specifically limit *de novo* synthesis of both fatty acids and cholesterol.

TLRs selectively reprogram lipid metabolism

Perturbations in fatty acid and cholesterol homeostasis have been observed in response to a number of viral and microbial infections, leading us to ask if signaling through immune receptors could influence the cellular programs that regulate lipid homeostasis in macrophage. To test this idea, we measured metabolic flux through the *de novo* lipid biosynthetic program via ^{13}C isotope enrichment studies [16] on bone marrow derived macrophage (BMDMs). To that end, BMDMs were cultured with 50% U^{13}C-labelled glucose in complete media supplemented with 5% FBS stimulated with type I interferon (IFNβ) or various Toll-like Receptor (TLR) agonists (TLR2: Pam3CSK4, TLR3: PolyIC, TLR4: LPS) representative of an array of pathogen-associated molecular patterns (PAMPs). Isotope enrichment analysis demonstrated that signaling through IFNAR and TLRs can markedly influence synthesized and total lipid pools, and a PAMP-specific manner (Figure 1A & B). TLR2 stimulation with Pam3CSK4 resulted in a modest, but significant increase in synthesis of palmitic acid (16:0), stearic acid (18:0) and cholesterol by 48hr (Figure 1A). This increase was accompanied by an increase in total cellular palmitic acid, stearic acid and cholesterol (Figure 1B), suggesting that signaling through TLR2 can enforce both lipid synthesis and scavenging programs. Conversely, TLR3 and IFNAR stimulation significantly

decreased the amount of synthesized palmitic acid, stearic acid and cholesterol over 48h (Figure 1A). Despite this significant attenuation of lipid biosynthesis, Poly:IC and IFNβ stimulation increased total cellular lipid levels similar to unstimulated counterparts (Figure 1B), indicating that these cells were also increasing lipid import. Consistent with our MS studies, we observed a significant increase in the uptake of dil-acetylated LDL in response to Poly:IC or IFNβ stimulation in BMDMs (Figure 1C). These results suggest that TLR3 and IFNAR signaling specifically reprogram cholesterol homeostasis in two ways: 1) by limiting flux through the lipid biosynthesis pathways, and 2) by shifting lipid homeostasis towards a scavenging program, resulting in maintenance of total cellular lipid content [11,16]. TLR4 stimulation resulted in a mixed phenotype. LPS treatment did not alter synthesis of palmitic acid, but modestly reduced synthesis of stearic acid and cholesterol after 48h (Figure 1A). Similar to TLR2 stimulation, TLR4 stimulation significantly increased total lipid content by 48h post stimulation (Figure 1B).

To determine if an active viral infection could influence the balance of lipid synthesis versus import, we infected BMDMs with murine gammaherpes virus-68 (MHV-68) for 48h in media with 50% $U^{13}C$-labelled glucose and supplemented with 5% FBS. Infection of BMDMs with MHV-68 significantly limited synthesis of palmitic acid, stearic acid and cholesterol synthesized over 48h, similar to IFN and PolyIC treatment (Figure 2A). Importanly, MHV-68 infection did not limit total lipid content (Figure 2B), suggesting that viral infection promotes a lipid import program while concurrently limiting lipid synthesis. Infection with MHV-68 engages a robust type I interferon response, leading us to hypothesize that changes in the lipid metabolism associated with viral infection may be mediated through IFNAR. To test this idea, we infected BMDMs with MHV-68 in the presence of IFNAR neutralizing antibodies. IFNAR blockade abrogated MHV-68 mediated changes in lipid synthesis and total lipids (Figure 2A and 2B), indicating that production of type I interferon was responsible for viral-mediated shifts in lipid metabolism.

Lastly, we considered the possibility that the availability of environmental lipids would influence IFN-mediated reprogramming. To address this, we cultured BMDMs with increasing percentages of serum (5, 10 and 20%) before stimulation with IFNβ. ISA modeling indicated that type I IFN treatment consistently decreased *de novo* synthesis of cholesterol and increased import to nearly the same extent in all serum conditions (Figure 3). Thus, we conclude that type I IFN signals reprogram the balance of lipid synthesis and import within a macrophage, but do not appear to specifically limit cholesterol and long chain fatty acid availability.

IFNAR signaling alters gene expression of lipid synthesis and scavenging genes

To better understand how IFNAR and TLR signaling altered lipid synthesis, we analyzed the gene expression of key enzymes involved in *de novo* lipid biosynthesis. Activation of TLR2 modestly and transiently repressed the expression of some cholesterol and fatty acid synthesis genes at 4h (Figure 4A); however, consistent with our biochemical analysis of synthesized lipids, TLR2 stimulation significantly upregulated the expression of key lipid synthesis enzymes by 24h (Figure 4B). TLR3 and IFNAR stimulation dramatically decreased expression of lipid synthesis genes by 4h post treatment, and maintained similar levels of repression at 24h post stimulation (Figure 4A and B). In line with this data, found that TLR3 and IFNAR stimulation significantly reduced Fatty Acid Synthase and Squalene Epoxidase protein levels (Figure 4C). Again, LPS treatment resulted in an intermediate phenotype, where lipid synthesis genes were repressed dramatically by 4h post stimulation, but by 24h the repression was not to the same extent as Poly:IC or IFNb treatment (Figure 4A and B). Finally, stimulation with flagellin, a potent TLR5 agonist, produced similar results to TLR2 stimulation (Figure 4A and B). In sum, this data suggests that TLR-mediated alterations in flux through the lipid biosynthetic pathways occur at least partially at the level of gene expression.

Of the TLRs we examined, only activation of TLR3 and TLR4 can lead to the rapid induction of *Ifnb1* expression (Figure 5A), leading us to hypothesize that repression of the fatty acid and cholesterol synthesis genes may converge on signaling through IFNAR. In line with this idea, recent studies indicate that type I IFNs can downregulate cholesterol biosynthesis genes [52-54], thus we asked if this inflammatory axis was necessary to induce the lipid metabolic reprogramming driven by TLR3/4 signaling. Genetic deletion of the IFNAR significantly abrogated repression of the lipid anabolic gene program by TLR3/4 at 24h post stimulation, indicating a requirement for the production of type I IFNs in this system (Figure 5B). TLR4 stimulation activates both TRIF (toll-like receptor adaptor molecule 1; Ticam1) and MYD88 (myeloid differentiation primary response gene) signaling cascades, but only signaling through TRIF results in rapid production of IFNβ. In line with an IFNAR-dependent mechanism, loss of TRIF, but not MYD88, abrogated TLR4-mediated repression of lipid synthesis genes (Figure 5C). Of note, TLR4 stimulation was still capable of ~30% repression at 4h post stimulation even in the absence of IFNAR (Figure 5D), similar to the degree of repression observed at 4h post TLR2 stimulation (Figure 4A). This suggests that there may be alternate signaling pathways outside of IFNAR that can transiently influence the lipid biosynthetic gene program, but may not be able to induce long-term repression of metabolic flux through the lipid biosynthetic programs.

Next, we examined the expression pattern of genes involved in cholesterol and fatty acid synthesis and import in MHV-infected BMDMs. We observed that infection decreased expression of genes encoding enzymes of the *de novo* cholesterol and fatty acid biosynthetic pathways (Figure 5E), similar to previous studies on cholesterol synthesis using cytomegalovirus [53]. MHV infection also significantly increased expression of Macrophage Scavenger Receptor (*Msr1*), a gene involved in lipid import (Figure 5E). Stimulation of BMDMs with IFNβ, LPS or Poly:IC for 24h also induced the expression of *Msr1* (Figure 5F). Importantly, blocking IFNAR signaling abrogated reprogramming of lipid metabolism driven by either MHV-

68 infection or type I IFN stimulation (Figure 5E and F). Of note, LPS-mediated induction of *Msr1* expression was only partially reduced by loss of IFNAR signaling (Figure 5F), suggesting that other aspects of downstream TLR4 signaling can also influence *Msr1* gene expression. This data suggests that type I IFN signals reprogram the balance of lipid synthesis and import within a macrophage, but do not specifically limit cholesterol and long chain fatty acid availability. In sum, we conclude that reprogramming of lipid anabolic metabolism by viral infection and TLR3/4 signals is dependent on the rapid production of type I IFNs, and subsequent signaling through IFNAR.

Rapid repression of lipid synthesis is Ch25h-independent

The enzyme Cholesterol 25-hydroxylase (*Ch25h*) is an interferon-stimulated gene (ISG) recently implicated in inflammatory responses and anti-viral immunity [53-55,62]. Ch25h enzymatically produces 25-hydroxycholesterol (25HC), an oxysterol that negatively regulates expression of lipid biosynthesis genes through its ability to bind the INSIG (insulin induced gene 1 and 2) proteins, and subsequently inhibit the sterol regulatory element binding proteins (SREBP1 and 2) [63]. We posited that the production of 25HC induced by type I IFNs could inhibit SREBP processing, resulting in downregulation of target genes (e.g., *Fasn*, *Sqle*). In agreement with published data [53-55,62], *Ch25h* expression was strongly induced by TLR3, TLR4 and IFNβ treatment of WT macrophages (Figure 6A). Unexpectedly, *Ch25h*$^{-/-}$ macrophages retained their ability to downregulate *Fasn* and *Sqle* at both 4 and 24h time points in response to IFNβ, LPS or Poly:IC (Figure 6B and C). Thus, we conclude that the reprogramming of lipid metabolism in response to TLR3/4 and type I IFN signals is not dependent on the induction of *Ch25h*.

Repression occurs at the level of transcription in STAT2-dependent manner

Canonical IFNAR signaling results in phosphorylation of JAK1 (Janus kinase 1) and Tyk2 (Tyk2). Activation of these kinases results in recruitment and activation of signal transducers

and activators of transcription (STATs), including STAT 1 and STAT2. STAT1 can either homodimerize (STAT1/STAT1) or heterodimerize with STAT2 (STAT1/STAT2). Upon IFNAR activation, STAT1 and STAT2 are phosphorylated, allowing them to translocate to the nucleus and upregulate numerous interferon stimulated genes. To determine if these transcription factors were needed for lipid synthesis repression, we stimulated BMDMs from STAT2 KO mice or J2-immortalized STAT1 KO BMDMs with IFNβ, PolyIC or LPS. Loss of either STAT2 or STAT1 was able to abrogate repression of the lipid synthesis genes (Figure 7A and B). Moreover, we find that long term STAT1-deficeincy conferred heightened basal levels of lipogenic genes (Figure 7B), suggesting that STAT1 signaling is required to set basal expression levels of lipid metabolic genes in macrophage.

The rapidity with which IFNAR signaling could downregulate the expression of lipid biosynthetic genes (Figure 8A)), and the observation that deletion either STAT1 or STAT2 could abrogate repression (Figure 7A and B), raised the possibility that repression may occur directly at the level of transcription. To address this, we assessed expression levels of unspliced nascent transcripts encoding lipid biosynthesis genes from either unstimulated or IFNβ treated BMDMs. Consistent with our mRNA studies, both *Fasn* and *Sqle* unspliced transcripts were significantly reduced by 2h after IFNβ treatment in WT BMDMs (Figure 8B). In contrast, STAT2 KO macrophages could not downregulate unspliced transcripts of fatty acid and cholesterol biosynthetic genes (Figure 8B). Consistent with this data, RNA-seq analysis 2h after TLR4 activation indicated that chromatin-associated nascent transcripts [64] were reduced in WT and MYD88-/- BMDMs, but not TRIF-/- or IFNAR-/- BMDMs (Figure 8C).

STAT1/2 transcription factors positively regulate upwards of 500 genes in response to IFNAR signaling. Thus, it remained possible that STAT1/2 signaling may have a secondary effect on lipid synthesis through transactivation of another target gene. To determine if a second round of

translation post IFNAR/STAT1/2 activation was required to repress lipid synthesis genes, we treated BMDMs with cyclohexamide, a potent inhibitor of translation, during interferon stimulation. Strikingly, 30 minute interferon treatment was able to repress unspliced transcripts of lipid synthesis genes to the same extent, regardless of cyclohexamide treatment (Figure 8D). This data suggests that STAT1/2 play a direct role in repressing lipid synthesis genes, perhaps acting as direct transcriptional repressors. Taken together, these data support a model where rapid downregulation of lipid synthesis by TLR3/4 requires induction of type I IFNs resulting in transcriptional repression of cholesterol and fatty acid biosynthesis genes in a STAT1/2-dependent manner. Furthermore, our data indicate that STAT1/2 signaling can reprogram the genetic cassette responsible for the maintenance of the lipid biosynthetic program regardless of lipid availability (Figure 3), suggesting that IFNAR/STAT2 signaling can override canonical transcription factors that regulate this pathway, perhaps by removal/displacement of these factors from the promoters (see Figure 8E for model).

Discussion and Future directions

In this study we demonstrate that decreasing *de novo* cholesterol and fatty acid synthesis is a physiologic response to activation of specific pathogen recognition receptors that engage IFNAR signaling (Figure 1A). One potential explanation for this rapid and specific reprogramming of lipid metabolism is that it may serve to limit the availability of lipid metabolites for invading pathogens. However, our metabolic flux studies also indicate that these same pro-inflammatory signals increase the total cellular pool size of cholesterol and long chain fatty acids, presumably to ensure sufficient lipid metabolite availability during activation induced cellular growth and effector function of macrophages. Thus, we conclude that the purpose of type I IFN-mediated reprogramming of lipid metabolism is to change the “set point” controlling the balance of these pathways, rather than to decrease lipids pool sizes *per se*. These data also suggest

that limiting intracellular lipid metabolite availability (e.g., cholesterol) for pathogen utilization is a less likely explanation for why interferon signals downregulate *de novo* lipid biosynthesis.

Our data indicate that downregulation of both cholesterol and fatty acid biosynthesis gene program occurs rapidly in response to IFNAR signaling. We can find significant decreases in primary transcript levels of lipid synthesis genes within only 30 minutes of IFNAR stimulation (Figure 8D). Additionally, we find the repression of lipid synthesis genes to be dependent on STAT1 and STAT2 transcription factors (Figure 7A and B). Importantly, repression of the lipid synthesis genes occurs independently of translation, indicating that the observed transcriptional repression is not caused by the expression of the secondary interferon gene (Figure 8D).

The SREBP family of transcription factors are capable of activating the entire cassette of lipid synthesis genes, leading us to hypothesize that STAT1/2 may directly influence the promoters of these genes either by blocking SREBP nuclear import, or removing SREBPs from the promoters of these genes. Chromatin Immuno-Precipitation (ChIP) assays will be required to determine if SREBP promoter occupancy of the lipid synthesis genes is altered. SREBPs have also been shown to require other transcription factors, specifically SP1 or NFY, for maximal transcriptional activity [65,66]. Thus, it is also possible that STAT1/2 may influence SP1 or NFY promoter occupancy in addition to SREBP. Both STAT1 and STAT1/2 heterodimers have largely been shown to positively regulate interferon-stimulated genes through their ability to bind to ISREs and GAS elements respectively, and subsequently trans-activate interferon stimulated target genes (e.g., antiviral and inflammatory genes- designated ISGs) [67]. Negative regulation of gene expression by STAT proteins is less well understood. A requirement for STAT1 in the repression of a few genes, including c-myc, in response to IFN-gamma stimulation has been noted, but the exact mechanism of STAT1-mediated repression remains unclear [68-70]. It will be important in our future studies to determine if STAT1/2 heterodimers can directly bind to the

promoter regions of lipid synthesis genes, causing a direct change in promoter occupancy of SREBPs or other general transcription machinery.

Furthermore, our data shows that lipogenic genes have sustained repression IFNAR signaling (e.g., 48h after Poly:IC and IFNβ treatment; data not shown). This repression is maintained despite negative regulation of IFNAR signaling at this time point (data not shown), leading us to hypothesize that remodeling of the epigenetic state of promoters is part of a mechanism to maintain long-term repression of lipid anabolism. Thus, future experiments accessing the levels of H3K27me3, H3K4me4, H3K9ac, and H3K18ac chromatin marks within the promoters of the lipid synthesis genes will also be important. The idea that epigenetic markers can maintain long-term silencing of lipid genes highlights that possibility that alterations in macrophage lipid metabolism may be part of a trained immunity program to ensure lasting pathogen memory in specific subsets of macrophage, such as resident tissue macrophage (Figure 9).

Since IFNAR/STAT signaling is obligatory for antiviral immunity, we hypothesized that interferon-mediated attenuation of lipid biosynthesis is an important component of host defense to viral infection. While deletion of IFNAR, STAT1 or STAT2 abolished lipid metabolic reprogramming in response to type I interferon, deletion of these factors also abolishes ISG expression required for antiviral immunity. Thus, to better understand the involvement of lipid metabolic reprogramming in response to type I interferon, we will need to create a genetic model mimicking transcriptional repression of lipid synthesis (see Chapter 3). Lastly, while much of this study has focused on IFNAR-dependent repression of lipid synthesis, we also observed that TRL2 stimulation enhanced lipid synthesis (Figure 1A). Future studies will be required to determine the role of enhanced lipid synthesis in TLR2-mediated inflammation.

Experimental Procedures for Chapter 2

Mouse Strains: C57BL/6 (WT) were purchased from Jackson Labs. IFNAR KO mice were a kind gift from Dr. Ting-Ting Wu (UCLA).

Mouse cells: Bone marrow was differentiated into macrophages in DMEM containing 20% FBS (Omega), 5% M-CSF conditioned media, 1% pen/strep (Gibco), 1% glutamine (Invitrogen) 0.5% sodium pyruvate (Invitrogen) for 7-9 days prior to experimental use.

Viruses: Wild-type MHV-68 was purchased from ATCC. For all in vitro infection experiments, cells were infected with virus for 3 hours, then changed into fresh media.

Reagents: Cells were treated with LPS (Invivogen), mouse recombinant IFNβ (Biolegend), Poly:IC (Invivogen), and Pam3CSK4 (Invivogen). Doses indicated in figure legends.

Chromatin-attached RNA-seq: Macrophages were prepared as previously described in [71] from bone marrow of 6-week old male C57Bl/6 mice from the following strains: Control, *Myd88*-/-, *TRIF*-/- and *Ifnar*-/-. Adherent macrophages were stimulated on day 6 of culture. Chromatin-associated RNA was isolated as previously described in[64], and further purified by removing ribosomal RNA using the Life Technologies Ribominus Eukaryote kit. cDNA libraries were prepared using the Illumina Truseq v2 kit.

Immunoblots: Samples were normalized by cell number (Nexcelom K2 cell counting system) and lysed directly into 2x Lameli loading buffer. Protein extracts were separated on gradient 4% to 12% Bis–Tris SDS-PAGE gel (Invitrogen) and then transferred to a nitrocellulose membrane (Amersham). After blocking for 1 hour in a TBS containing 0.1% Tween 20 (TBST) and 5% nonfat milk, the membrane was probed with indicated antibodies diluted into TBST with 5% milk

overnight. Membranes were washed 4x with TBST, followed by a 30-minute room temperature incubation with secondary antibodies conjugated to horseradish peroxidase diluted in TBST plus 5% milk. Membranes were washed as before and then developed using Pierce ECL2 detection kit and imaged with Typhoon.

Antibodies: For Western Blots: FASN (Cell Signaling 3180), SQLE (Sigma AV42101), Actin (Santa Cruz sc-1616-R), For Blocking: Mouse IFNAR1 (Leinco I-400)

DiI-acLDL uptake: BMDMs were stimulated with 1000U/mL IFN or 2ug/mL Poly:IC for 48h in media containing 5% FBS. Cells were treated with DiI-acLDL (Invitrogen) at 1:200 dilution from manufacturer's stock solution directly into conditioned media for 2hr. BMDMs were washed 2x with PBS, lifted and optically counted with Nexcelom Cellometer. 1.5x10^5 cells per sample were lysed into 100uL RIPA Buffer (Boston Bioproducts) and spun at 15K in a bench top microfuge. 20uL of lysate was transferred to dark-walled, clear bottom 386 well dish and fluorescence intensity was measure with a typhoon (Amersham)

Gene expression analysis: RNA was extracted from all cells with Trizol using manufacturer's protocols. cDNA was synthesized with iScript cDNA Synthesis Kit (Bio-Rad) as per manufacturer's instructions (700ng/uL RNA per cDNA synthesis reaction). Quantitative PCR (qPCR) was conducted on the Roche LightCycler 480 using SYBR Green Master Mix (Kapa Biosciences) and 0.5 μmol/L primers. Relative expression values are normalized to control gene (36B4) and expressed in terms of linear relative mRNA values. Primer sequences are available upon request. When measuring HIV mRNA from infected cells, RNA was collected using Qiagen RNeasy Kit in combination with on-column DNAse treatment (Qiagen) prior to cDNA synthesis.

***Isotope Enrichment Experiments*:** Day 7 differentiated BMDMs in 24-well dishes (Wallac, Black Visiplate TC) were transferred to complete media containing 50% $U^{13}C$-glucose with or without 1000U/mL IFNβ , 2ug/mL Poly:IC, MHV-68 (MOI=0.5) or MHV +10ug/mL IFNAR Blocking antibody for 24/48hr before harvest. Immediately prior to collection, 1.25μM Calcein-AM (final concentration)(SantaCruz, sc-203865) was added to each well and incubated for 15 minutes. The plates were then imaged on a Molecular Devices ImageXpress XL. 21 high magnification fluorescence images were captured for each well (23.9% of total well surface area) using a 10x Objective (Nikon Plan Fluor, 0.3 NA). Cell number was assessed using MetaXpress Software with Powercore using the Multi-wavelength cell scoring module. Following imaging, cells are dissolved in 6M Guanidine HCl and transferred to glass tubes for derivitiziation with 3M methanolic guanidine HCl. Samples were prepared alongside standard curve samples made up of FAMES mix (Nu-chek Prep, GLC 20a) and Cholesterol (Sigma, C8667).

Total cellular fatty acids were prepared by mild acid methanolysis [72] with the following modifications: a total acid methanolysis reaction volume of 720μl was used with .6% HCl (w/v). 0.17μg of trinonadecanoin (Nu-chek Prep, T-165) and Stigmastanol (Sigma, S4297) were added to each reaction as internal standard for FAMES and Cholesterol analysis respectively. Following extraction of resulting FAMES and sterols with 1mL of hexane, 25ul of sample was analyzed for FAMES by GC/MS using an Agilent 7890B/5977A with DB-WAX column (Agilent, 122-7032). Complete GC-MS configurations and running programs available upon request. Sterols contained within remaining sample were derivatized with 5μl of anhydrous pyridine (Sigma, 270970) and 5μl BSTFA + TMCS, 99:1 (Sigma, 33155-U). 25ul of sample was run on Agilent 7890B/5977A with ZB-MR1 column (Zebron 7HG-G016-11).

Integration and quantification of all ions performed on MassHunter Quantitative Analysis Program (Agilent Technologies, B.06.00). Analysis for total quantification of Fatty Acids and

Cholesterol and relative contributions of synthesis to the respective pool over labeling period were determined by fitting the isotopologue distributions to Isotopomer Spectral Analysis (ISA) as previously described [16].

Chapter 2: Figure 1

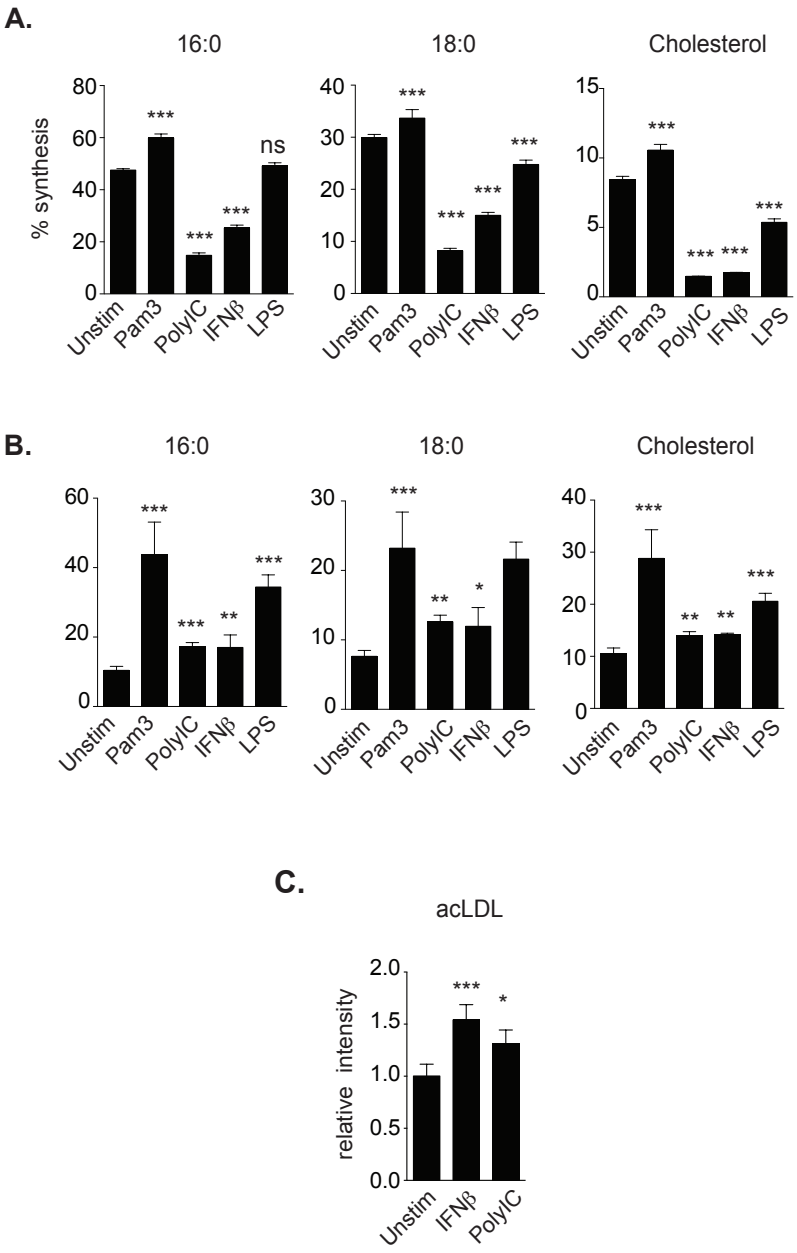

Chapter 2: Figure 1. TLR signaling shifts the balance of lipid synthesis and import. (A) Percent synthesis of palmitic acid (16:0) and cholesterol as measured by metabolic flux analysis in C57BL/6 bone marrow derived macrophages (BMDMs) with or without LPS (100ng/mL), Poly:IC (2ug/mL), Pam3CSK4 (200ng/uL Pam3) or interferonβ (1000U/mL IFNβ) stimulation for 48h. **(B)** Total cellular palmitic acid (16:0) and cholesterol from BMDMs stimulated as in (A). **(C)** Uptake of DiI-acLDL in BMDMs treated with IFNβ or Poly:IC as above. All experiments are reported as means ± SD from four independent experiments, unless noted otherwise. **P* < 0.05; ***P* < 0.01, ****P* < 0.005 (two-tailed unpaired Student's *t* test)

Chapter 2: Figure 2

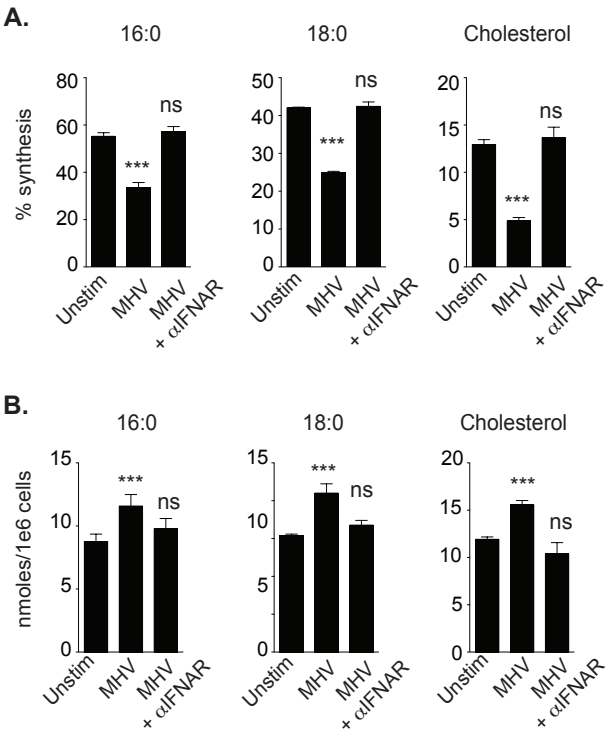

Chapter 2: Figure 2. Viral infection shifts the balance of lipid synthesis and import. (A) Percent synthesis of palmitic acid (16:0), stearic acid (18:0) and cholesterol as measured by Isotopic Spectral Analysis (ISA) on C75BL/6 BMDMs infected with MHV-68 (MOI=0.5) +/- 10ug/mL IFNAR neutralizing antibody for 48h. **(B)** Total cellular palmitic acid (16:0), stearic acid (18:0) and cholesterol from BMDMs stimulated as in (A). All experiments are reported as means ± SD from four independent experiments, unless noted otherwise. $*P < 0.05$; $**P < 0.01$, $***P < 0.005$ (two-tailed unpaired Student's *t* test)

Chapter 2: Figure 3

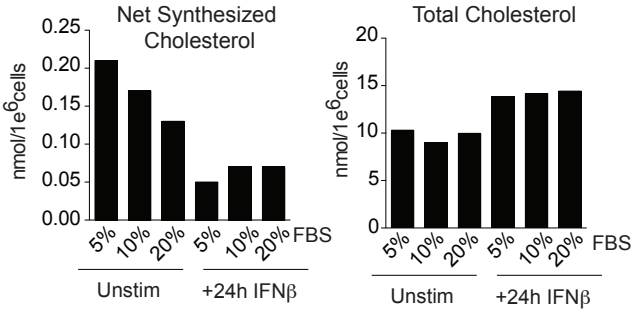

Chapter 2: Figure 3. Serum conditions do not alter type I interferon-mediated shifts in lipid metabolism. Net Synthesis of cholesterol as measured by ISA (left) and total cholesterol (right) from BMDMs +/- 1000U/mL IFNβ for 24h. Each bar represents an individual condition.

Chapter 2: Figure 4

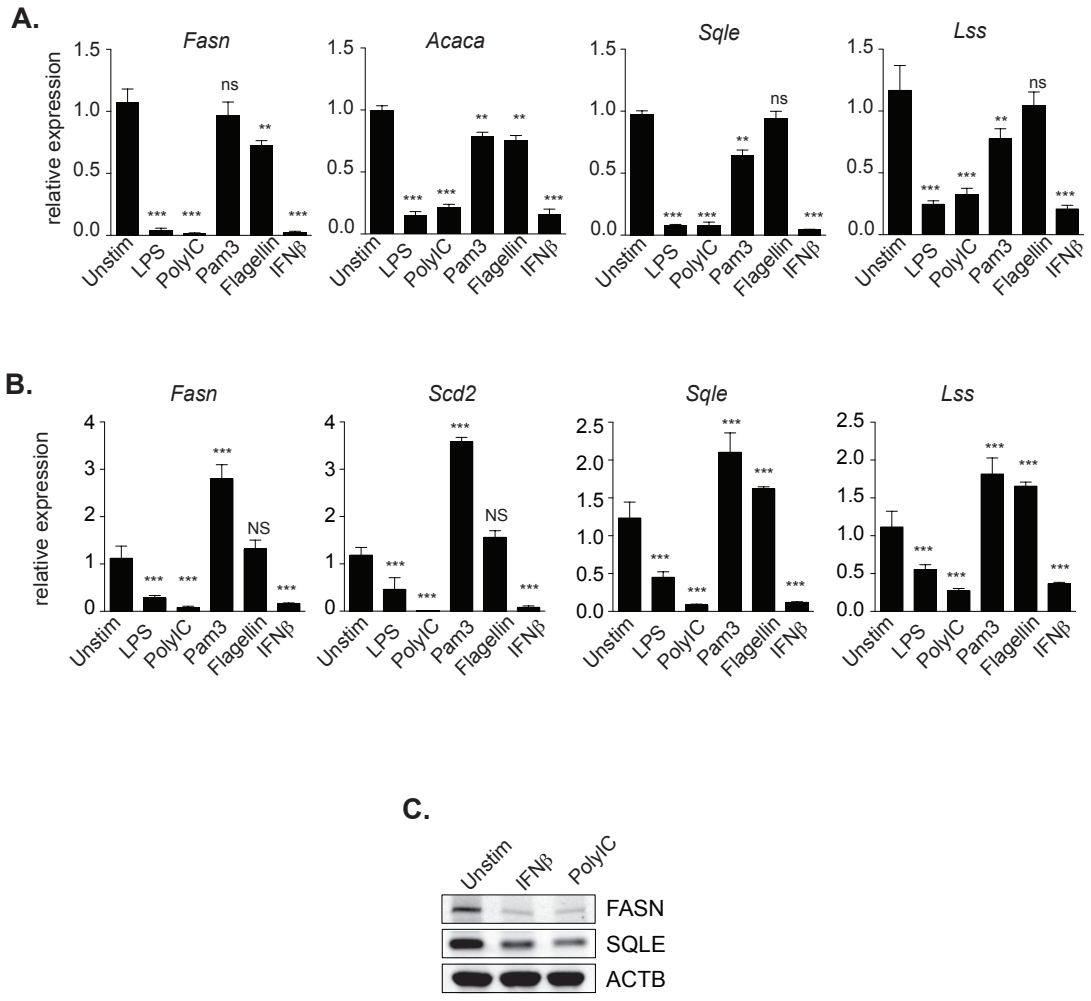

Chapter 2: Figure 4. TLRs influence expression of lipid synthesis genes. (A) qPCR analysis of indicated lipid biosynthesis genes in quiescent (Unstim) BMDMs or stimulated with LPS (100ng/mL), Poly:IC (2ug/mL), Pam3CSK4 (200ng/uL), Flagellin (100ng/mL) or interferonβ (1000U/mL IFNβ) for 4h. **(B)** qPCR analysis of indicated lipid biosynthesis genes in quiescent (Unstim) BMDMs or stimulated with LPS (100ng/mL), Poly:IC (2ug/mL), Pam3CSK4 (200ng/uL), Flagellin (100ng/mL) or interferonβ (1000U/mL IFNβ) for 24h. **(C)** Western blot analysis of FASN and SQLE in WT BMDMs unstimulated or stimulated with 1000U/mL IFNβ or 2ug/mL Poly:IC for 24h. All experiments are reported as means ± SD from three independent experiments, unless noted otherwise. $*P < 0.05$; $**P < 0.01$, $***P < 0.005$ (two-tailed unpaired Student's *t* test)

Chapter 2: Figure 5

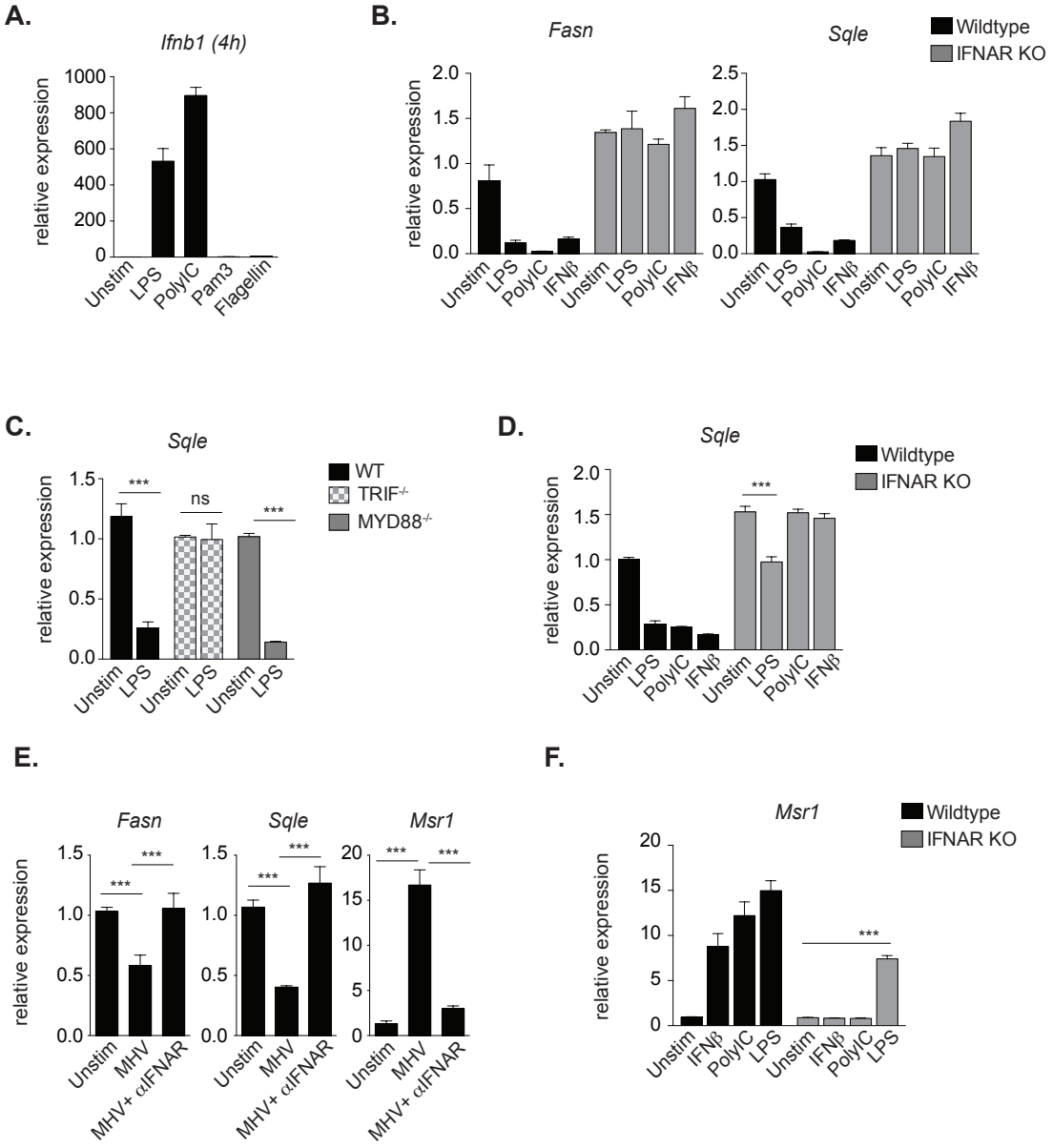

Chapter 2: Figure 5. Repression of lipid synthesis genes in response to TLR3/4 require IFNAR. (A) qPCR analysis of *Ifnb1* expression in response to LPS (100ng/mL), Poly:IC (2ug/mL), Pam3CSK4 (200ng/uL Pam3) or interferonβ (1000U/mL IFNβ) stimulation for 24h. **(B)** qPCR analysis of *Fasn* and *Sqle* gene expression in wildtype or *IFNAR KO* BMDMs unstimulated or stimulated with LPS, Poly:IC, or IFNβ as above for 24h **(C)** qPCR analysis of *Sqle* gene expression in wildtype, TRIF KO or MYD88 KO BMDMs unstimulated or stimulated with 200ng/uL LPS 24h. **(D)** qPCR analysis of *Fasn* and *Sqle* gene expression in wildtype or *IFNAR KO* BMDMs unstimulated or stimulated with LPS, Poly:IC, or IFNβ as above for 4h. **(E)** qPCR analysis of *Fasn*, *Sqle*, and *Msr1* gene expression in BMDMs infected with MHV-68 (MOI=0.5) +/- 10ug/mL IFNAR neutralizing antibody for 48h. **(F)** qPCR analysis of*Msr1* gene expression in WT or IFNAR KO BMDMs unstimulated or stimulated with 200ng/uL LPS, 1000U/mL IFNβ or 2ug/mL Poly:IC for 24h. All experiments are reported as means ± SD from three independent experiments, unless noted otherwise. **P* < 0.05; ***P* < 0.01, ****P* < 0.005 (two-tailed unpaired Student's *t* test)

Chapter 2: Figure 6

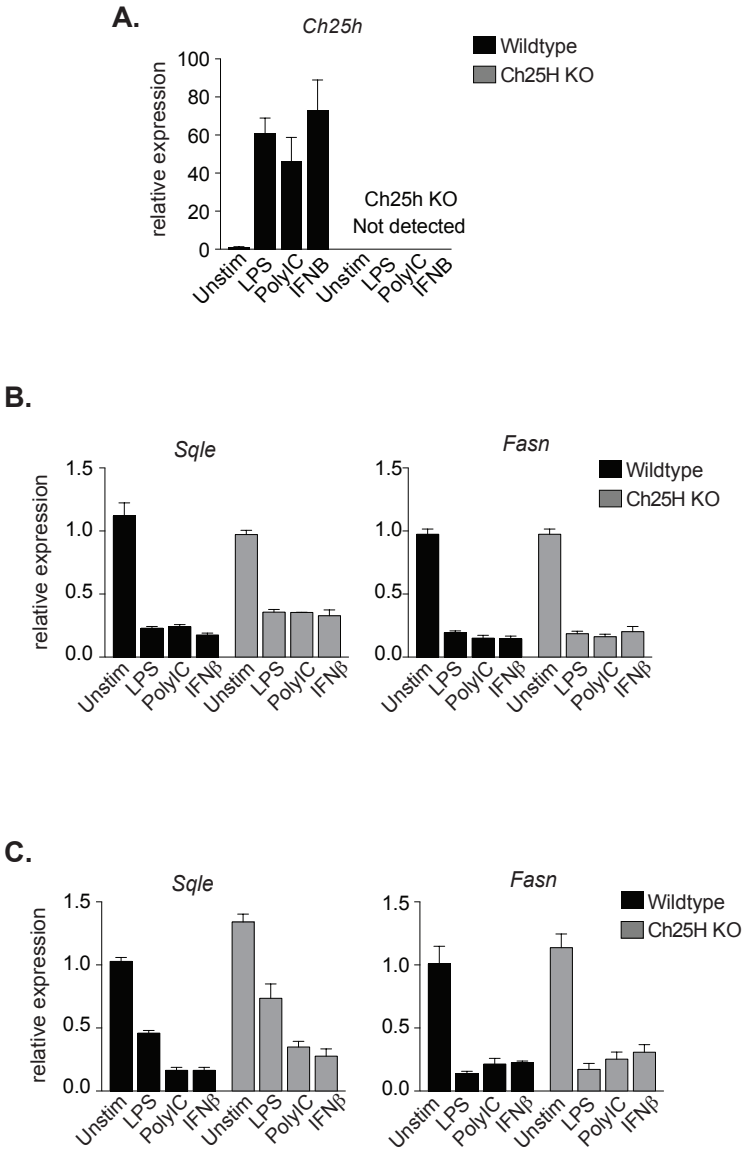

Chapter 2: Figure 6. Repression of lipid synthesis genes is independent of *Ch25h* expression. (A) *qPCR analysis of Ch25h expression in WT or Ch25h$^{-/-}$ BMDMs treated with* 100ng/mL LPS, 2ug/mL Poly:IC, or 1000U/mL IFNβ for 4h. **(B)** qPCR analysis of *Fasn* and *Sqle* expression in WT or CH25h$^{-/-}$ BMDMs treated as in (A) for 4h. **(C)** qPCR analysis of *Fasn* and *Sqle* expression in WT or CH25h$^{-/-}$ BMDMs treated as in (A) for 24h. All experiments are reported as means ± SD from three independent experiments, unless noted otherwise. **P* < 0.05; ***P* < 0.01, ****P* < 0.005 (two-tailed unpaired Student's *t* test)

Chapter 2: Figure 7

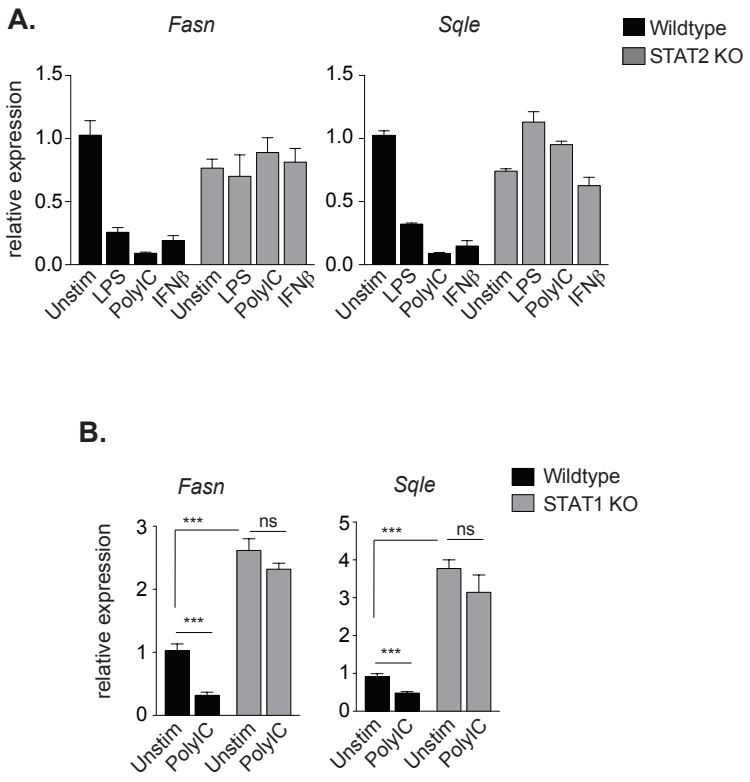

Chapter 2: Figure 7. Repression of lipid synthesis genes is dependent on STAT1/STAT2

(A) qPCR analysis of *Fasn* and *Sqle* gene expression in wild-type or *STAT2 KO* BMDMs unstimulated or stimulated with LPS, Poly:IC, or IFNβ as in Figure 1A for 24h. **(B)** qPCR analysis of *Fasn* and Sqle expression in WT or STAT1 KO J2-immortalized BMDMs stimulated with PolyIC for 4h. All experiments are reported as means ± SD from three independent experiments, unless noted otherwise. **P* < 0.05; ***P* < 0.01, ****P* < 0.005 (two-tailed unpaired Student's *t* test)

Chapter 2: Figure 8

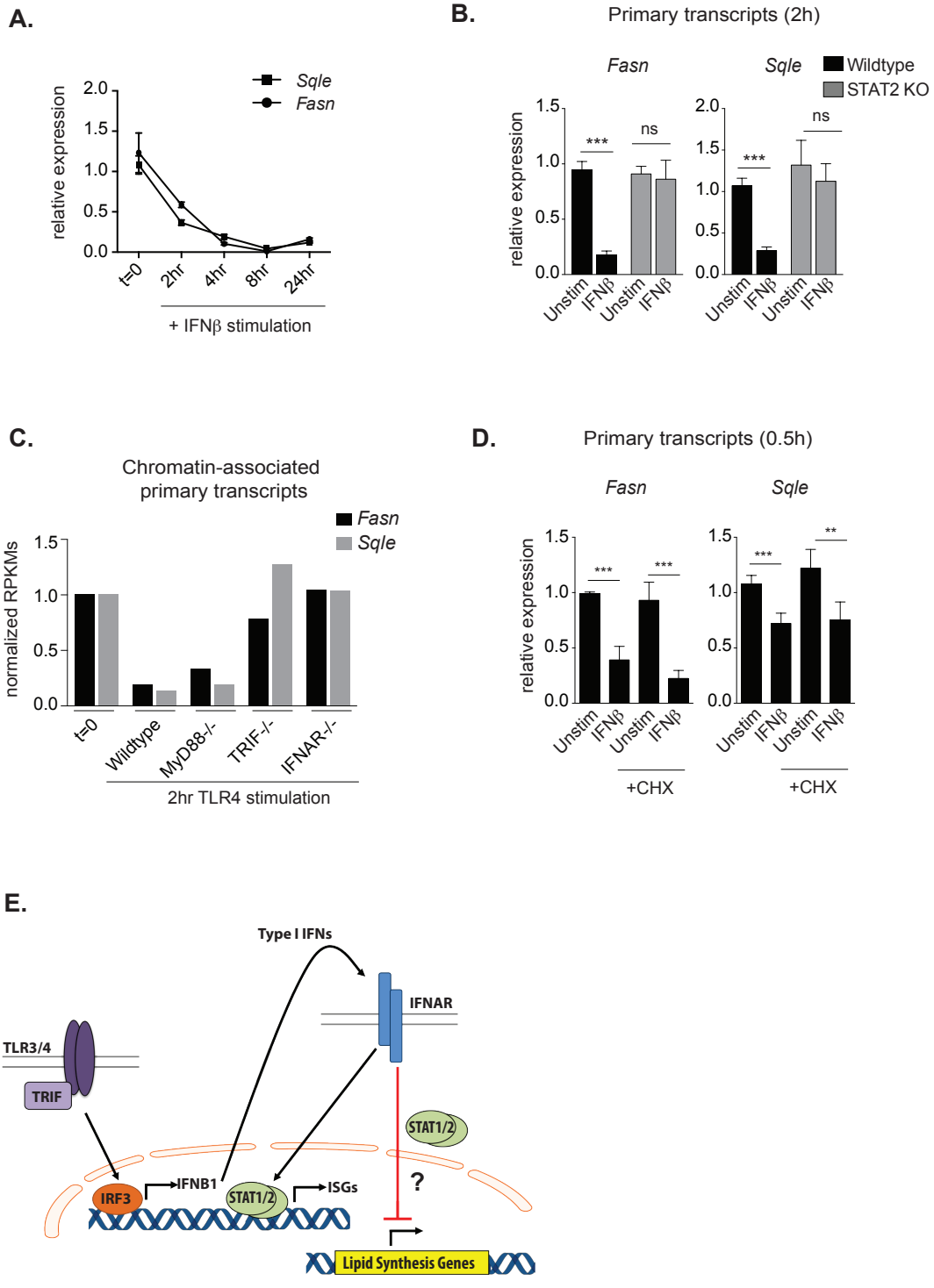

Chapter 2: Figure 8. Repression of lipid synthesis genes occurs at the level of transcription. (A) qPCR analysis of *Fasn* and *Sqle* expression time course in WT BMDM **(B)** qPCR analysis of unspliced, primary transcripts of *Fasn* and *Sqle* in wild-type or STAT2 KO BMDMs unstimulated or stimulated with IFNβ as in Figure 1A for 2h. **(C)** RNA-seq analysis of chromatin-attached nascent transcripts at T=0 or 2h after 100ng/mL Lipid A treatment in WT, MYD88 KO, TRIF KO or IFNAR BMDMs (average of two independent experiments). **(D)** qPCR analysis of unspliced, primary transcripts of *Fasn* and *Sqle* in wild-type BMDMs unstimulated or stimulated with IFNβ as in Figure 1A for 0.5h +/- 10ng/mL cyclohexaminde (CHX). **(E)** Schematic indicating that TLR3/4-mediated repression of the lipid synthesis genes occurs rapidly in an IFNAR-dependent manner at the level of transcription. Repression of lipid synthesis genes requires direct action of STAT1 and STAT2. All experiments are reported as means ± SD from three independent experiments, unless noted otherwise. **P* < 0.05; ***P* < 0.01, ****P* < 0.005 (two-tailed unpaired Student's *t* test)

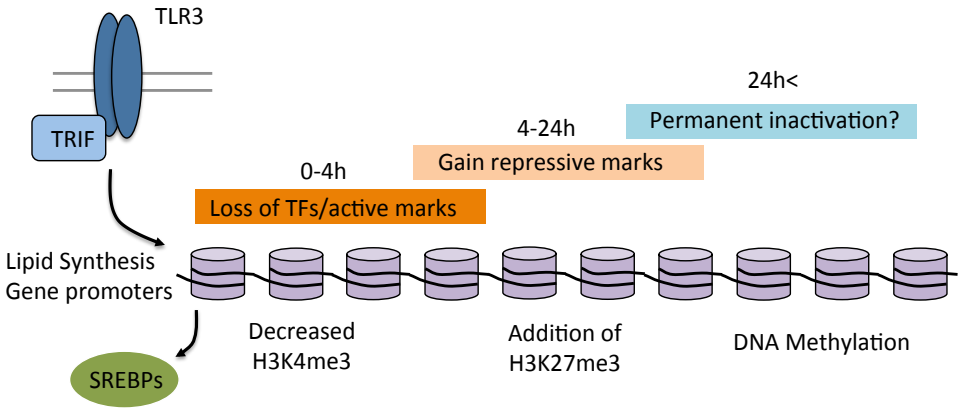

Chapter 2: Figure 9. A model for repression lipid synthesis genes by the TLR3 IFNAR signaling. We posit that initial decreases in gene expression will result from loss of transcription factors and Pol II accompanied by loss of active marks. Over time, we predict that sustained repression will be accompanied by addition of repressive marks and increased nucleosomes. Permanent reprogramming of metabolism has not been shown but could be mediated by DNA methylation and could underlie macrophage training.

References for Chapter 2:

11. Vance DE, Vance JE (2008) Biochemistry of lipids, lipoproteins and membranes. Amsterdam ; Boston: Elsevier. xii, 631 p., 638 p. of plates p.

16. Williams KJ, Argus JP, Zhu Y, Wilks MQ, Marbois BN, et al. (2013) An essential requirement for the SCAP/SREBP signaling axis to protect cancer cells from lipotoxicity. Cancer Res 73: 2850-2862.

22. Spann NJ, Garmire LX, McDonald JG, Myers DS, Milne SB, et al. (2012) Regulated accumulation of desmosterol integrates macrophage lipid metabolism and inflammatory responses. Cell 151: 138-152.

27. Castrillo A, Tontonoz P (2004) Nuclear receptors in macrophage biology: at the crossroads of lipid metabolism and inflammation. Annu Rev Cell Dev Biol 20: 455-480.

36. Coppens I (2013) Targeting lipid biosynthesis and salvage in apicomplexan parasites for improved chemotherapies. Nat Rev Microbiol 11: 823-835.

37. Baek SH, Li AH, Sassetti CM (2011) Metabolic regulation of mycobacterial growth and antibiotic sensitivity. PLoS Biol 9: e1001065.

38. Griffin JE, Pandey AK, Gilmore SA, Mizrahi V, McKinney JD, et al. (2012) Cholesterol catabolism by Mycobacterium tuberculosis requires transcriptional and metabolic adaptations. Chem Biol 19: 218-227.

39. Bard M, Sturm AM, Pierson CA, Brown S, Rogers KM, et al. (2005) Sterol uptake in Candida glabrata: rescue of sterol auxotrophic strains. Diagn Microbiol Infect Dis 52: 285-293.

40. Cui HL, Ditiatkovski M, Kesani R, Bobryshev YV, Liu Y, et al. (2014) HIV protein Nef causes dyslipidemia and formation of foam cells in mouse models of atherosclerosis. FASEB J 28: 2828-2839.

41. Greseth MD, Traktman P (2014) De novo fatty acid biosynthesis contributes significantly to establishment of a bioenergetically favorable environment for vaccinia virus infection. PLoS Pathog 10: e1004021.

42. Herker E, Ott M (2011) Unique ties between hepatitis C virus replication and intracellular lipids. Trends Endocrinol Metab 22: 241-248.

43. Ouellet H, Johnston JB, de Montellano PR (2011) Cholesterol catabolism as a therapeutic target in Mycobacterium tuberculosis. Trends Microbiol 19: 530-539.

44. Heaton NS, Perera R, Berger KL, Khadka S, Lacount DJ, et al. (2010) Dengue virus nonstructural protein 3 redistributes fatty acid synthase to sites of viral replication and increases cellular fatty acid synthesis. Proc Natl Acad Sci U S A 107: 17345-17350.

45. Kapadia SB, Chisari FV (2005) Hepatitis C virus RNA replication is regulated by host geranylgeranylation and fatty acids. Proc Natl Acad Sci U S A 102: 2561-2566.

46. Petersen J, Drake MJ, Bruce EA, Riblett AM, Didigu CA, et al. (2014) The major cellular sterol regulatory pathway is required for Andes virus infection. PLoS Pathog 10: e1003911.

47. Liu CI, Liu GY, Song Y, Yin F, Hensler ME, et al. (2008) A cholesterol biosynthesis inhibitor blocks Staphylococcus aureus virulence. Science 319: 1391-1394.

48. Munger J, Bennett BD, Parikh A, Feng XJ, McArdle J, et al. (2008) Systems-level metabolic flux profiling identifies fatty acid synthesis as a target for antiviral therapy. Nat Biotechnol 26: 1179-1186.

49. Parihar SP, Guler R, Khutlang R, Lang DM, Hurdayal R, et al. (2014) Statin therapy reduces the mycobacterium tuberculosis burden in human macrophages and in mice by enhancing autophagy and phagosome maturation. J Infect Dis 209: 754-763.

50. Rzouq F, Alahdab F, Olyaee M (2014) Statins and hepatitis C virus infection: an old therapy with new scope. Am J Med Sci 348: 426-430.

51. Gilbert C, Bergeron M, Methot S, Giguere JF, Tremblay MJ (2005) Statins could be used to control replication of some viruses, including HIV-1. Viral Immunol 18: 474-489.

52. Blanc M, Hsieh WY, Robertson KA, Watterson S, Shui G, et al. (2011) Host defense against viral infection involves interferon mediated down-regulation of sterol biosynthesis. PLoS Biol 9: e1000598.

53. Blanc M, Hsieh WY, Robertson KA, Kropp KA, Forster T, et al. (2013) The transcription factor STAT-1 couples macrophage synthesis of 25-hydroxycholesterol to the interferon antiviral response. Immunity 38: 106-118.

54. Liu SY, Aliyari R, Chikere K, Li G, Marsden MD, et al. (2013) Interferon-inducible cholesterol-25-hydroxylase broadly inhibits viral entry by production of 25-hydroxycholesterol. Immunity 38: 92-105.

55. Reboldi A, Dang EV, McDonald JG, Liang G, Russell DW, et al. (2014) Inflammation. 25-Hydroxycholesterol suppresses interleukin-1-driven inflammation downstream of type I interferon. Science 345: 679-684.

56. Funk JL, Feingold KR, Moser AH, Grunfeld C (1993) Lipopolysaccharide stimulation of RAW 264.7 macrophages induces lipid accumulation and foam cell formation. Atherosclerosis 98: 67-82.

57. Keyel PA, Tkacheva OA, Larregina AT, Salter RD (2012) Coordinate stimulation of macrophages by microparticles and TLR ligands induces foam cell formation. J Immunol 189: 4621-4629.

58. Dushkin MI, Kovshik GG (2013) Effect of toll-like receptor agonists on the formation of macrophage/foam cells upon acute peritonitis in mice. Bull Exp Biol Med 156: 49-52.

59. Huang YL, Morales-Rosado J, Ray J, Myers TG, Kho T, et al. (2014) Toll-like receptor agonists promote prolonged triglyceride storage in macrophages. J Biol Chem 289: 3001-3012.

60. Koberlin MS, Snijder B, Heinz LX, Baumann CL, Fauster A, et al. (2015) A Conserved Circular Network of Coregulated Lipids Modulates Innate Immune Responses. Cell.

61. Huang SC, Everts B, Ivanova Y, O'Sullivan D, Nascimento M, et al. (2014) Cell-intrinsic lysosomal lipolysis is essential for alternative activation of macrophages. Nat Immunol 15: 846-855.

62. Shibata N, Carlin AF, Spann NJ, Saijo K, Morello CS, et al. (2013) 25-Hydroxycholesterol activates the integrated stress response to reprogram transcription and translation in macrophages. J Biol Chem 288: 35812-35823.

63. Du X, Pham YH, Brown AJ (2004) Effects of 25-hydroxycholesterol on cholesterol esterification and sterol regulatory element-binding protein processing are dissociable: implications for cholesterol movement to the regulatory pool in the endoplasmic reticulum. J Biol Chem 279: 47010-47016.

64. Bhatt DM, Pandya-Jones A, Tong AJ, Barozzi I, Lissner MM, et al. (2012) Transcript dynamics of proinflammatory genes revealed by sequence analysis of subcellular RNA fractions. Cell 150: 279-290.

65. Naar AM, Beaurang PA, Robinson KM, Oliner JD, Avizonis D, et al. (1998) Chromatin, TAFs, and a novel multiprotein coactivator are required for synergistic activation by Sp1 and SREBP-1a in vitro. Genes Dev 12: 3020-3031.

66. Reed BD, Charos AE, Szekely AM, Weissman SM, Snyder M (2008) Genome-wide occupancy of SREBP1 and its partners NFY and SP1 reveals novel functional roles and combinatorial regulation of distinct classes of genes. PLoS Genet 4: e1000133.

67. Ivashkiv LB, Donlin LT (2014) Regulation of type I interferon responses. Nat Rev Immunol 14: 36-49.

68. Ramana CV, Grammatikakis N, Chernov M, Nguyen H, Goh KC, et al. (2000) Regulation of c-myc expression by IFN-gamma through Stat1-dependent and -independent pathways. EMBO J 19: 263-272.

69. Sharma B, Iozzo RV (1998) Transcriptional silencing of perlecan gene expression by interferon-gamma. J Biol Chem 273: 4642-4646.

70. Sibinga NE, Wang H, Perrella MA, Endege WO, Patterson C, et al. (1999) Interferon-gamma-mediated inhibition of cyclin A gene transcription is independent of individual cis-acting elements in the cyclin A promoter. J Biol Chem 274: 12139-12146.

71. Ramirez-Carrozzi VR, Braas D, Bhatt DM, Cheng CS, Hong C, et al. (2009) A unifying model for the selective regulation of inducible transcription by CpG islands and nucleosome remodeling. Cell 138: 114-128.

72. Ichihara K, Fukubayashi Y (2010) Preparation of fatty acid methyl esters for gas-liquid chromatography. J Lipid Res 51: 635-640.

CHAPTER 3:

Limiting Cholesterol Biosynthetic flux engages type I interferon-mediated antiviral immunity

Introduction

In our previous work, we found that signaling through type I interferon receptor (IFNAR) rapidly down regulated the genes the genes involved in fatty acid and cholesterol biosynthesis in a STAT1/2-dependent manner. In line with this data, type I interferon (IFN) dramatically reduced the contribution of synthesis of both fatty acids and cholesterol without limiting total pool sizes of cellular lipids. This data led us to hypothesize that specifically limiting lipid synthesis may be a novel aspect of the type I IFN response, and may be important for antiviral immunity. To directly address this question this would require a genetic model where the "set point" controlling the balance of lipid synthesis and scavenging was shifted independent of IFNAR signaling. To accomplish this, we generated mice with macrophage-specific deletion of the SREBP cleavage-activating protein (SCAP) using the LysM-Cre model. SCAP is an endoplasmic reticulum (ER) sterol-sensing protein required to chaperone the sterol regulatory element binding proteins (SREBP1 and SREBP2) [19]. In the absence of SCAP protein, SREBP1 and 2 transcriptional activities are significantly attenuated, resulting in markedly reduced expression of cholesterol and fatty acid biosynthesis genes (see Figure S1A for schematic and reviewed Chapter 1) [17].

Loss of SREBP activity shifts the balance of lipid synthesis and import in BMDMs

Gene expression analysis of bone marrow-derived macrophages (BMDMs) confirmed that genetic deletion of SCAP markedly decreases expression of the genes encoding enzymes of the *de novo* cholesterol and fatty acid biosynthetic programs (Figure 1A). However, loss-of-SCAP does not appear to influence the *in vitro* differentiation of BMDMs (Figure S1B), nor impact the frequency of macrophages or other immune cell populations in LN, spleen and bone marrow (Figure S1C). Next, we performed ^{13}C-isotope enrichment and ISA to determine if loss-of-SCAP altered lipid biosynthetic capacity. To that end, control, control/IFNβ-treated (24h), and SCAP$^{-/-}$ macrophages were cultured in complete media containing U^{13}C-labelled glucose and 5% FBS. As expected, IFNβ treatment markedly decreased cholesterol and fatty acids synthesis

in control macrophages (Figure 1B). Importantly, the contribution of synthesis to total lipid pools in SCAP$^{-/-}$ macrophages was similar to that of IFNβ-treated control BMDMs (Figure 1B, S1D). Total cholesterol and fatty acid pool sizes were similar between IFNβ-treated control and SCAP$^{-/-}$ BMDMs (Figure 1C), demonstrating that loss-of-SCAP does not significantly decrease the total amounts of these lipids in BMDMs. Taken together, these data demonstrate that SCAP-deficiency phenocopies the shift in lipid homeostasis observed in response to IFNβ stimulation without requiring TLR3 agonist or exogenous type I IFNs.

Loss of SCAP protects from viral inflection

Next, we sought to determine if genetically enforcing this metabolic shift in macrophages influenced host defense. To begin investigating this, control and SCAP$^{-/-}$ BMDMs were infected with MHV-68 for 48h. Examination of viral gene expression revealed that SCAP$^{-/-}$ BMDMs contained significantly lower viral transcripts (Figure 2A), indicative of lower viral burden. Similarly, stable knockdown of *SCAP* in human THP1 macrophages rendered cells resistance to HIV-1, decreasing HIV-1 RNA and p24 protein expression by approximately 70% at 96h after infection (Figure 2B). To determine if macrophage-specific perturbations in the lipid biosynthetic program could influence viral pathogenesis *in vivo*, LysM-Cre$^{+/-}$ and LysM-Cre$^{+/-}$/Scap$^{fl/fl}$ mice were challenged intranasally with MHV-68 ($5e^3$ PFU). Similar to our *in vitro* results, we found that the loss-of-SCAP in macrophages alone was sufficient to reduce viral load in lungs by over 90% (Figure 2C). Taken together, our data indicates that genetic deletion of SCAP can be protective in viral inflections, and supports the concept that lipid metabolic reprogramming can be a protective component of host response to viral infections.

Loss of SCAP primes a type I IFN response

MHV replicates in a number of cell types including macrophages, type 1 and type 2 pneumocytes [73], leading us to hypothesize that viral resistance conferred by loss-of-SCAP in

macrophages may be transferable to neighboring cells. To directly test this, conditioned media (C.M.) from naïve control or SCAP$^{-/-}$ macrophages was collected and transferred to wildtype (C57BL/6) BMDM cultures for a 4h incubation period before challenge with MHV-68 (MOI=0.5, see Figure S2A for schematic). Remarkably, transfer of SCAP$^{-/-}$ conditioned media to WT BMDM cultures was able to reduce MHV-68 viral burden by approximately 50% at 48h post-infection (Figure 2D). These results indicate that the viral resistance phenotype observed in SCAP-deficient macrophages occurs, at least in part, through the production of secreted factors that then prime cells for anti-viral immunity.

Type I IFNs are secreted proteins that have an essential role in anti-viral immunity, leading us to ask if genetic deletion of SCAP influenced type I IFN responses. Gene expression studies on unstimulated BMDMs revealed that loss-of-SCAP results in the spontaneous induction of a type I IFN-inflammatory response characterized by heightened *Ifnb1* and interferon-stimulated genes (ISGs, e.g., *Mx1, Mx2, Irf7, Ccl2, Cxcl10*) (Figure 2E). Heightened ISG expression was also observed in alveolar macrophages collected by bronchoalveolar lavage from LysM-Cre$^{+/-}$/Scap$^{fl/fl}$ (Figure 2F, S2B), indicating that loss-of-SCAP drives a type I IFN signature *in vivo*. Addition of IFNAR blocking antibody to BMDM cultures was able to abrogate ISG expression (Figure 2G), suggesting that SCAP$^{-/-}$ macrophage spontaneously produce more type I IFNs. In support of this, transfer of culture supernatants from unstimulated SCAP$^{-/-}$ BMDMs to quiescent WT macrophages was able to induce an ISG signature (Figure 2H). Additionally, we observed the upregulation of a type I IFN signature in human THP1 macrophages in response to either stable or transient silencing of SCAP (Figure S2C, S2D), indicating that this signaling axis is conserved. Importantly, addition of IFNAR blocking antibody abrogated antiviral capacity of conditioned media from SCAP$^{-/-}$ BMDMs (Figure 2I), supporting the concept that the anti-viral effect of SCAP-deficiency was, in large part, mediated through production of type I IFNs.

Next, we asked if the change in basal inflammatory response observed in SCAP-deficient macrophages would result in priming of the inflammatory response to TLR stimulation. To that end, control and SCAP$^{-/-}$ macrophages were stimulated with LPS, Poly:IC and type I IFNs. We observed that both human and mouse SCAP-deficient macrophages have significantly heightened induction of *Ifnb1* and ISGs in response to both LPS and Poly:IC, as well as type I IFN treatment (Figure 2J left, S2E-G). Interestingly, not all inflammatory responses were upregulated in SCAP-deficient macrophages. We found that induction of *Il1b*, a canonical pro-inflammatory factor downstream of TLR4 activation, was significantly attenuated in response to LPS (Figure 2J, right). IFNAR blockade was able to partially restore upregulation of *Il1b* expression in TLR4 stimulated SCAP-deficient macrophages (Figure S2H), indicating that type IFN signaling contributes, in part, to repression of *Il1b* in LPS stimulated cells. Taken together, these data indicate that reprogramming of lipid metabolism can prime macrophages for heightened IFN responses to PAMPs or cytokine signals, however this type of metabolic reprogramming also entrains specific inflammatory responses at the expense of other inflammatory programs.

Induction of a type I IFN signature segregates with loss of SREBP2

SCAP is required for activation of all isoforms of the SREBP transcription factors. In mammals there are two SREBP genes that express three SREBP proteins. SREBP1a and SREBP1c are produced via alternative transcriptional start sites on *SREBF1*, whereas the *SREBF2* gene encodes SREBP2 [19]. In general, SREBP1 activates transcription of genes involved in fatty acid synthesis, while SREBP2 is responsible for transcriptionally activating genes required for cholesterol synthesis (schematic Figure S1A). Thus, we sought to determine if the spontaneous induction of inflammation observed in SCAP-deficient macrophages was dependent on loss of the SREBP1 or SREBP2 transcriptional axis. To that end, we generated THP1 macrophages stably expressing shRNA targeting either *SREBF1* or *SREBF2* (designated herein as

shSREBP1 or shSREBP2, respectively) and performed RNA-sequencing studies on unstimulated macrophages. As expected, knockdown of SREBP1 attenuated expression of genes involved in fatty acid synthesis, whereas loss of SREBP2 decreased expression of cholesterol biosynthesis genes (Figure S3A, S3B). Bioinformatic analysis of RNA-seq data indicted that heightened expression of ISGs, and enrichment of pathways involved in host defense to viral infection, segregated entirely with the loss of SREBP2 expression (Figure 3A and S3C). qPCR analysis confirmed that silencing of SREBP2 in primary human PBMC-derived macrophages or THP1 cells resulted in heightened basal expression of *IFNB1* and an interferon gene signature (Figure 3B, S3D, S3E). In line with this pro-inflammatory phenotype, SREBP2-deficient macrophages were significantly resistant to Influenza A and HIV-1 challenge (Figure 3C, S3F). In contrast, a type I IFN signature was not observed in shSREBP1 macrophages (Figure 3A, 3B and S3E), indicating that the spontaneous induction of type I interferon-mediated inflammation occurs specifically in response to genetically perturbing the SCAP/SREBP2 pathway.

Nearly every cell in the body has the ability to produce type I IFNs, thus we sought to determine if genetic deletion of SREBP2 in non-immune cells would also result in the spontaneous induction of a type I IFN signature and resistance to viral challenge. To that end, we examined the basal expression levels of ISGs from SREBP2-null mouse embryonic fibroblasts (designated SREBP2$^{-/-}$ MEFs). Similar to our studies in macrophages, we observed that SREBP2$^{-/-}$ MEFs constitutively expressed heightened levels of *Ifnb1* and ISGs (Figure 3D), and IFNAR blockade significantly reduced ISG expression to that of control MEFs (Figure 3E). Correspondingly, SREBP2$^{-/-}$ MEFs were significantly resistance to MHV-68 challenge (Figure 3F), and produced heightened ISGs in response to MHV infection (Figure 3G). Importantly, pretreatment with IFNAR-neutralizing antibodies was sufficient to abrogate the heightened anti-viral immunity

observed in SREBP2$^{-/-}$ MEFs (Figure 3H), indicating that the anti-viral immunity seen in SREBP2-deficient cells is largely dependent on IFNAR signaling.

Limiting flux through the mevalonate pathway engages a type I IFN response

Mevalonate Kinase Deficiency (MKD) is an autosomal recessive disease caused by significantly decreased enzymatic activity of mevalonate kinase [74,75]. Interestingly, those individuals with moderate residual enzymatic activity (~20% of wildtype) are characterized by recurrent episodic fevers, persistent inflammatory responses and hyper IgD production (termed Hyperimmunoglobulinemia D with Periodic Fever Syndrome or HIDS). SREBP2 has a well-defined role in transcriptionally regulating the enzymes involved in the mevalonate pathway [19], leading us to ask if MKD results in the spontaneous generation of type I IFN-mediated inflammation. Examination of primary fibroblasts from an individual with MKD revealed heightened basal ISG expression when compared to population controls (Figure 4A). Genetic silencing of mevalonate kinase (*MVK*) or HMG-CoA reductase (*HMGCR*), the rate-limiting enzyme in cholesterol biosynthesis, in macrophages also resulted in the upregulation of *IFNB1* and ISGs (Figure 4B, S4A, S4B). In contrast, silencing of stearoyl-CoA desaturase 1 (*SCD1*), a key enzyme involved in flux through the long-chain fatty acid biosynthetic pathway [16], did not induce ISGs (Figure S4A, S4C). Importantly, we also find that MKD fibroblasts are primed for exaggerated type I IFN-mediated inflammatory responses. Activation of MKD fibroblasts with Poly:IC resulted in a significantly heightened ISG signature after 24h (Figure 4C). Taken together, these data indicate that decreasing flux through the mevalonate pathway results in the upregulation of a type I IFN response, and provides a potential mechanistic explanation for the inflammatory symptoms and immune dysregulation observed in individuals with MKD.

ISG signature in response to changes in mevalonate flux is LXR-independent

Intermediary metabolites of cholesterol biosynthesis have been shown to activate the Liver X Receptors (LXRα and β), nuclear receptors with a clear role in repressing lipid-driven metabolic inflammation [7,9,22,23]. Consistent with this, we found that LXR target genes *ABCA1* and *IDOL* were significantly decreased in both SREBP2- and SCAP-deficient macrophages (Figure 4D). Thus, we considered the possibility that the upregulation of *IFNB1* and downstream ISGs resulted from decreased LXR signaling. However, treatment of SREBP2-deficient macrophages with LXR ligand GW3965, which restored LXR function (Figure S4D), failed to reduce expression of ISGs (Figure 4E). These findings indicate that LXRs do not repress type I IFN-mediated inflammation, and are in agreement with previous work [76].

Replenishing free cholesterol attenuates the type IFN-signature in SREBP2 null cells

In combination, our data demonstrate that decreasing flux through the mevalonate pathway induces type I IFN-mediated inflammation, leading us to ask if replenishing cholesterol could attenuate this inflammatory program. To this end, control and SREBP2-deficient macrophage cultures were treated with methyl-beta-cyclodextrin conjugated cholesterol (MβCD-cholesterol) to supplement free cholesterol levels in loss-of-function cells. Supplementing SREBP2-deficient macrophages with MβCD-cholesterol significantly reduced the expression of ISGs (Figure 4F). Thus, we conclude that restoring cholesterol homeostasis alone is sufficient to abrogate the induction of a type I IFN signature in cells that have the mevalonate pathway perturbed. Consistent with this, replenishing cholesterol in SREBP-deficient BMDMs abrogated the anti-viral phenotype (Figure 4G). In combination, these data suggest that acutely decreasing synthesized cholesterol appears to provide a novel “danger” signal that activates a type IFN – mediated anti-viral response.

IRF3 links perturbations in cholesterol homeostasis to *Ifnb1* transcription

Finally, we sought to define the molecular mechanism linking perturbations in cholesterol biosynthesis with the spontaneous induction of type I interferon-mediated inflammation. We had observed that IFNAR blockade reduced ISG expression (Figure 2G, 3E), but was not able to decrease *Ifnb1 gene* expression in both SCAP- and SREBP2-deficient cells (Figure 5A left, S5A). However, addition of MβCD-cholesterol was able to reduce the expression level of *Ifnb1* (Figure 5A right, S5B), supporting a model where induction of inflammation in SREBP2- or SCAP-deficient cells is dependent on transcriptional upregulation of type I IFNs. Interferon Regulatory Factor 3 and 7 (IRF3 and IRF7) are transcription factors with well-defined roles in the transcriptional regulation of *Ifnb1* [77,78]. We observed that SREBP2-deficeint cells had significantly elevated expression of IRF7 (Figure 2E, 3A, 5B), leading us to ask if IRF7 was important in mediating inflammation. To address this, we transiently silenced *Irf3* or *Irf7* in SREBP2$^{-/-}$ MEFs (Figure 5B). We observed that silencing of *Irf7* was able to partially reduce ISG expression (Figure 5C), but had no influence on *Ifnb1* expression (Figure 5C, left). In contrast, silencing of *Irf3* completely abrogated *Ifnb1* expression and correspondingly attenuated ISG expression (Figure 5C). Taken together, these data indicate that IRF3 is required to drive the spontaneous upregulation of *Ifnb1* and ISGs observed in SREBP2-deficeint cells, and that IRF7 serves to amplify the ISG program.

STING links changes in cholesterol synthesis with IFNβ production

Stimulator of Interferon Genes (STING; *TMEM173*) and Mitochondrial Antiviral-Signaling (*MAVS*) pathways are known to facilitate IRF3 nuclear translocation and upregulation of *Ifnb1* transcription in response to cytosolic dsDNA or ssRNA, respectively [79-82]. To determine if these pathways were contributing to IRF3 activation and *Ifnb1* expression, we silenced MAVS or STING in SREBP2-deficient cells. Silencing of MAVS had no effect on heightened *Ifnb1* and ISG expression in SREBP2-deficient MEFs (Figure 5D, S5C). In contrast, silencing of STING

completely abrogated heightened *Ifnb1* and ISG expression in MEFs and macrophages (Figure 5D, 5E S5C-G). STING ligands (cyclic di-nucleotides) can be generated by the enzymatic activity of cGAMP synthase (cGAS; *Mb21d1*). Gene expression studies revealed that SREBP2-deficeint cells have basally heightened expression of cGAS (Figure S5C), which is partially dependent on STING, IRF3 and IFNAR signaling (Figure S5C, S5H, S5I). Transiently silencing cGAS reduced the expression of *Ifnb1* and ISGs in SREBP2-deficient cells to that of controls, indicating that heightened STING activity observed in SREBP2$^{-/-}$ cells is dependent on generation of endogenous STING ligands (Figure 5F).

Perturbations in cholesterol homeostasis alters STING sensitivity to cyclic di-nucleotides

STING is an endoplasmic reticulum (ER)-resident protein that functions as a scaffold that promotes phosphorylation of TANK-binding kinase 1 (TBK1) and IRF3 in response to cyclic di-nucleotides [80]. Western blot analysis demonstrated increased basal phospho-TBK1 in SREBP2-defcieint MEFs (Figure 6A). Silencing of *Tbk1* alone was sufficient to reduce expression of *Ifnb1* and ISGs (Figure 6B) in SREBP2$^{-/-}$ cells. Likewise, silencing of STING or cGAS attenuated heightened pTBK1 (Figure 6C). Taken together, these data confirm a requirement for the cGAS/STING/TBK1/IRF3 signaling axis in linking changes in cholesterol metabolism with induction of *Ifnb1*.

We posited that addition of exogenous cholesterol should reduce signaling activity through the STING/TBK1 pathway. Replenishing cholesterol to SCAP$^{-/-}$ BMDMs significantly reduced phospho-TBK1 levels (Figure 6D), whereas IFNAR blockade had no significant effect on pTBK1 (Figure 6A, 6D). These data suggest that cholesterol levels directly influence the ability of STING to transduce signals to TBK1. To address this, control and SCAP$^{-/-}$ BMDMs were treated with a low dose of exogenous STING ligand (cyclic di-GMP (herein denoted as “cGMP”)-5ug/mL) for 45 minutes. We observed that cGMP treatment significantly increased pTBK1 levels

in SCAP$^{-/-}$ BMDMs compared to that of controls (Figure 6E). Importantly, addition of cholesterol to these cells markedly diminished cGMP induced *Ifnb1* expression (Figure 6F). Taken together, these data support a model where perturbations in cholesterol biosynthetic flux intrinsically influence STING/TBK1 responsiveness to cyclic di-nucleotides, and provides a molecular mechanism linking cholesterol homeostasis with type I IFN-mediated inflammation (see model Figure 7).

Discussion and future directions

In this study, we identify a metabolic-inflammatory circuit that is an important component of host defense to pathogens. We initially show that rapidly decreasing *de novo* cholesterol and fatty acid biosynthesis is a physiologic response to viral infection and activation of IFNAR signaling pathways, in agreement with other recently published gene expression studies [52,55] (see Chapter 2, Figure 1A). One potential explanation for this rapid reprogramming of cholesterol and fatty acid biosynthesis is that it may serve to limit the amount of lipid macromolecules available to invading pathogens. However, our metabolic flux studies also indicate that these same pro-inflammatory signals increase the total cellular pool size of cholesterol and long chain fatty acids, presumably to ensure sufficient lipid metabolite availability during activation induced cellular growth and effector function of macrophages. Thus, we conclude that the purpose of type I IFN-mediated reprogramming of lipid metabolism is to change the "set point" controlling the balance of these pathways, rather than to decrease lipids pool sizes *per se*. These data also suggest that limiting intracellular lipid metabolite availability (e.g., cholesterol) for pathogen utilization is a less likely explanation for why interferon signals downregulate *de novo* lipid biosynthesis. Rather, our data indicates that selectively decreasing flux through the cholesterol biosynthetic pathway engage the type I IFN response and primes cells for heightened anti-viral immunity. In this way, IFN signaling decreases cholesterol biosynthesis and in a reciprocal manner, acutely decreasing cholesterol biosynthesis drives type I IFN responses. Therefore, we conclude that

the mevalonate pathway and IFN-signaling pathway are part of a metabolic-inflammatory circuit that ensures any changes in the activity of one pathway are sensed by the other pathway (Figure 7). Identification of this circuit furthers our mechanistic understanding of how lipid metabolism and inflammation are intertwined, and could provide insights as to how these pathways become dysregulated in both metabolic and inflammatory diseases.

We also show that genetically repressing flux through the mevalonate pathway can serve to prime cells for heightened type I IFN inflammatory responses when challenged with TLR3, TLR4 or type I IFNs. We find this to be true in fibroblasts from individuals who are mevalonate kinase hypomorphs, and confirm these results in WT cells by genetically silencing enzymes in this pathway. These data could help to mechanistically explain why individuals with Mevalonate Kinase Deficiency exhibit heightened inflammatory responses and have episodic fevers. It may also shed light on the enigmatic relationship between pharmacologic inhibitors of cholesterol biosynthesis (e.g., Statins- which target HMG-CoA reductase) and protection from viral and bacterial infections. While this category of drugs have been shown to be protective in a number of infections, the molecular mechanisms are unclear, and have been attributed to a wide range of on-target and off-target effects. These include directly influencing pathogen replication or survival, limiting egress from the cells by perturbing host lipid availability, and finally, anti-inflammatory effects on host cells [49-51,83]. Given that type I IFNs can both potentiate certain types of inflammatory responses through the genetic regulation of a large cassette of host defense genes, while negatively regulating others inflammatory pathways (e.g. IL-1β) [84], suggests that a potential explanation for the pleotropic effects of statins is via engagement of a subclinical type I IFN response. In support of this notion, recent studies by Cyster and colleagues observed that acute deletion of SCAP in macrophages decreases IL1β production [55]. We also observe this in our system (Figure 2J), and we predict that while acutely decreasing lipid biosynthesis favors anti-viral responses, it may also render the host more

susceptible to other classes of infections that require inflammasome activity for protective inflammatory responses.

One striking implication of our data is that synthesized lipids convey unique information about cellular status despite being chemically indistinguishable from their imported counterparts. One of the simplest explanations for this observation is that *de novo* synthesized lipids are initially partitioned into the ER bilayer before being distributed to subcellular pools or the plasma membrane [19]. In contrast, lipid import occurs at the plasma membrane and must transit through a number of cellular processing/transport pathways before reaching the ER or other organelles [12,15]. As such, subcellular concentration of a specific lipid species would convey information regarding cellular metabolic homeostasis. Indeed, this is the operating principle underlying the tight regulation of the SREBP pathway, where ER sterol content is monitored by the SCAP and INSIG proteins [13,85]. STING protein is in also embedded in the ER membrane [79], thus we propose a model where the STING signaling axis is activated in response to decreasing the ER bilayer cholesterol pool size. Moreover, given that all nucleated cells have the ability to synthesize cholesterol and that STING is expressed in a wide variety of cell types, we predict that this metabolic inflammatory circuit is likely to exist in a broad array of tissues.

As to how perturbations in the pool size of synthesized cholesterol directly engages the STING pathway remains unclear at this time. We find that there remains a requirement for cGAS, indicating that the generation of STING ligand is still a necessary component. We considered the possibility that perturbing flux through the cholesterol biosynthetic pathway could significantly increase intracellular levels of STING ligands [81]. However, cGAMP levels in both control and SREBP2-deficient cells remained below our limits of detection by LC-MS (~240 fmole; data not shown [86,87]). Thus, we believe it unlikely that changes in cholesterol are significantly altering the levels of STING ligands in cells. Thus, we propose a model where

decreasing cholesterol levels in the ER membrane facilitate STING/TBK1 interactions. In this system, STING from SREBP2-deficient cells would respond more efficiently to the same amount of cGAS-produced ligand, thus explaining the requirement for cGAS for enhanced IFNβ production in SREBP2-deficient cells. In line with this, we find that SREBP2-deficient cells have increased sensitivity to stimulation with cyclic di-nucleotides, resulting in heightened TBK1 phosphorylation. Furthermore, addition of cholesterol to SREBP2-deficient cells was sufficient to decrease phosphorylation of TBK1 in support of the notion that cholesterol levels influence STING/TBK1 interaction. Of course, it remains possible that cholesterol is also regulating the function of other components of this signaling axis (e.g., cGAS or TBK1) and it will be important in future studies to mechanistically address these questions.

Finally, our observation that cholesterol pool size can be monitored by host defense machinery raises the intriguing possibility that other classes of lipids are also monitored through yet to be defined sensor-signaling pathways. Indeed, our data indicates that IFNAR signaling can also limit flux through the *de novo* fatty acid biosynthetic program (See Chapter 2, Figure 1A), but the immunological consequences of this observation still remain unclear. Further experiments will be required to elucidate the signaling pathways involved in shaping the lipid “codes” enforced by innate immune receptors and to fully appreciate the role of lipid metabolic reprogramming during the innate immune response. In conclusion, the studies presented herein provide mechanistic insights as to how perturbations in cholesterol homeostasis engage inflammatory pathways, and advance our understanding of the crosstalk between lipid metabolism and host defense.

Experimental Procedures for Chapter 3:

Mouse Strains: C57BL/6, B6;129-*Scap*^{tm1Mbjg}/J and LysM-Cre$^{+/-}$ *were purchased from* Jackson Labs. IFNAR KO mice were a kind gift from Dr. Ting-Ting Wu (UCLA). B6;129-*Scap*^{tm1Mbjg}/J were crossed with LysM-Cre$^{+/-}$ mice to obtain LysM-Cre$^{+/-}$SCAP$^{fl/fl}$.

Human Cell lines: THP1 cells were obtained from Dr. Scott Kitchen (UCLA, Department of Medicine) and cultured in RPMI media with 10% FBS (Omega Scientific) with penicillin/streptomycin (Gibco). THP1 cells were differentiated with phorbol 12-myristate 13-acetate (PMA) at 50ng/mL (EMD Millipore) for 48-96hrs depending on the experiment. For viral infection studies, THP1 cells were differentiated for 72h prior to infection.

Primary Human cells: Human monocyte-derived macrophage: Peripheral blood mononuclear cells (PBMCs) were isolated from leukopacks using standard ficoll procedures. Monocytes were separated from PBMCs via plastic adherence. Monocytes were differentiated into macrophage with 10ng/mL human M-CSF (Biolegend) in RPMI (Gibco) media with 10% FBS for 7 days prior to experimental use. Human primary fibroblasts from MVK-deficient (Catalog# GM12014) or population controls (Catalog# ND38530) were obtained from Coriell Institute for Medical Research and cultured under recommended conditions.

Mouse cells: Bone marrow was differentiated into macrophages in DMEM containing 20% FBS (Omega), 5% M-CSF conditioned media, 1% pen/strep (Gibco), 1% glutamine (Invitrogen) 0.5% sodium pyruvate (Invitrogen) for 7-9 days prior to experimental use. WT and SREBP2$^{-/-}$ MEFs were obtained from Dr. Karen Reue (UCLA). MEFs were cultured in DMEM plus 10% FBS with 1% Pen/Strep unless noted otherwise.

Viruses: HIV1 was produced by transfecting 293T cells with $pHIV_{89.6}$ using lipofectamin 2000 (Life Technology) according to the manufacturer's protocol. $HIV1_{89.6}$ was harvested 2 d after transfection and purified with 0.22um filter and quantified by p24 ELISA. Influenza A/WSN/33 (H1N1) was produced by transfecting 293T cells with the 8-plasmid reverse genetics system [88]. Wild-type MHV-68 was purchased from ATCC. For all in vitro infection experiments, cells were infected with virus for 3 hours, then changed into fresh media.

Reagents: Cells were treated with MBCD-Cholesterol (Sigma), GW3965 (Sigma), LPS (Invivogen), human recombinant IFNa (Fitzgerald), mouse recombinant IFNβ (Biolegend), Poly:IC (Invivogen), c-di-GMP (Invivogen) and RIG-I agonist 5'ppp RNA (Invivogen). Doses indicated in figure legends.

Genetic Manipulation: Commercial short hairpin RNAs (shRNA) were obtained from Sigma. Lentiviruses were generated using 3rd generation system with puromyocin selection (plasmids available upon request). Plasmids were transfected with either Lipofectamine 2000 (Invitrogen) or DNAfectin 2100 (Lambda Biosciences). Small Interfering RNAs (siRNAs) were purchased from Dharmacon/Thermo (product numbers: Control: J-012808-05-0002, Human SCAP: J-012808-05-0002, Mouse STING: J-055528-06-0005, Mouse MAVS: J-053767-05-0005, Mouse cGAS: J-055608-10-0005, Mouse IRF3: J-041095-06-0005, Mouse IRF7: J-041094-05-0005). THP1 cells were differentiated for 2 days with 50ng/mL PMA before siRNA transfection (3e5 cells/well into 12 well dishes). siRNAs (40nM final) were transfected using Lipofectamine RNAiMAX and Optimem (Invitrogen) using manufacturer's instructions. Cells were harvested 72hrs after transfection for protein or RNA. MEFs were plated at 7.5e4 cells per well in 6 well dishes in DMEM containing 10% FBS. siRNAs (40nM final) were transfected Lipofectamine RNAiMAX and Optimem (Invitrogen) using manufacturer's instructions. 24 hrs post transfection, cells were put into fresh DMEM containing 1% FBS for 48hr.

CRISPR targeting of STING (TMEM173) in THP1 cells: STING was targeted with CRISPR-Cas9 using a lentivirus expressing a gRNA and Cas9-T2A cassette (including a sequence encoding a protein for resistance to puromycin) as previously described[89]. THP1 cells were transduced with lentivirus and selected with 5μg/ml puromycin (Life Technologies). The *TMEM173* gRNA target sequence is 5'-GGTGCCTGATAACCTGAGTA-3'.

Antibodies: For Western Blots: MX1 (Abcam ab95926), Actin (Santa Cruz sc-1616-R), HIV p24 (Abcam ab9071), STING (Cell Signaling 3337S), TBK1 (Cell Signaling 3013), phopho-TBK1 (Cell Signaling 5483). For Blocking: Mouse IFNAR1 (Leinco I-400) and Human IFNAR (Millipore MAB1155)

Immunoblots: Samples were normalized by cell number (Nexcelom K2 cell counting system) and lysed directly in RIPA Buffer before 1:1 dilution with 2x Lameli loading buffer. Protein extracts were separated on gradient 4% to 12% Bis–Tris SDS-PAGE gel (Invitrogen) and then transferred to a nitrocellulose membrane (Amersham). After blocking for 1 hour in a TBS containing 0.1% Tween 20 (TBST) and 5% nonfat milk, the membrane was probed with indicated antibodies diluted into TBST with 5% milk overnight. Membranes were washed 4x with TBST, followed by a 30-minute room temperature incubation with secondary antibodies conjugated to horseradish peroxidase diluted in TBST plus 5% milk. Membranes were washed as before and then developed using Pierce ECL2 detection kit and imaged with Typhoon.

Gene expression analysis: RNA was extracted from all cells with Trizol using manufacturer's protocols. cDNA was synthesized with iScript cDNA Synthesis Kit (Bio-Rad) as per manufacturer's instructions (700ng/uL RNA per cDNA synthesis reaction). Quantitative PCR (qPCR) was conducted on the Roche LightCycler 480 using SYBR Green Master Mix (Kapa Biosciences) and 0.5 μmol/L primers. Relative expression values are normalized to control gene (36B4) and expressed in terms of linear relative mRNA values. Primer sequences are available

upon request. When measuring HIV mRNA from infected cells, RNA was collected using Qiagen RNeasy Kit in combination with on-column DNAse treatment (Qiagen) prior to cDNA synthesis.

RNA-Seq method: RNA was purified using Qiagen RNeasy Kit and submitted to the UCLA Clinical Microarray Core for RNA-seq analysis. Total RNA was first enriched for mRNA with NEB NEBNext Poly(A) mRNA Magnetic isolation kit. The mRNA samples were then put on WaferGen Apollo 324 system for automated library preparation using WaferGen PrepX™ RNA-Seq Library reagent kit for Illumina. Library products were next enriched through PCR and multiplexing barcodes were also added. Sequencing was performed on Illumina HiSeq 2000 for a pair end 100 run. Data quality check was done on Illumina SAV. Demultiplexing was performed with Illumina CASAVA 1.8.2 and fastq files were generated.

RNA-Seq Data Analysis*:* The STAR aligner (v2.3.0 [90]) was used to generate the genome index and perform alignments. The index was built using the GRCh37 assembly (hg19) of the human genome and the corresponding junction database from Ensemble's gene annotation. RNA-Seq reads were then aligned in paired-end mode. Relevant alignment parameters include: minimum alignment similarity = 0.75, minimum alignment length relative to read length = 0.66, score range to define multiple alignments = 0.66, and maximum ratio of mismatches to read length = 0.1. On average, 90% of the reads were reported as uniquely mapped. Alignment outputs were used to generate the gene-level count matrix with HTSeq-count v0.6.1p2[91] in "*intersection-nonemtpy"* mode, keeping only protein coding loci from the Ensembl genome annotation. DESeq v1.14.0 [92] was used for normalization (using the geometric mean across samples), differential expression (to classify genes as differentially expressed, Benjamini-Hochberg adjusted p-value < 0.01) and to compute moderate expression estimates by means of a variance-stabilized transformation. Differentially expressed genes were subjected to model-based clustering [93]to classify genes by their overall expression profile across all conditions

(shControl, shSREBP1 and shSREBP2 cells), and functional annotations of selected clusters were retrieved from WebGestalt [94] (see Figure S4c). Heatmap in Figure 3A was built with GENE-E (http://www.broadinstitute.org/cancer/software/GENE-E/) applying relative min/max normalization to moderate expression estimates. Expression estimates in units of RPKMs (reads per kilobase of mappable gene length and million of aligned reads) were computed using in-house scripts.

***Isotope Enrichment Experiments*:** Day 7 differentiated BMDMs in 24-well dishes (Wallac, Black Visiplate TC) were transferred to complete media containing 50% $U^{13}C$-glucose with or without 1000U/mL IFNβ , 2ug/mL Poly:IC, MHV-68 (MOI=0.5) or MHV +10ug/mL IFNAR Blocking antibody for 24/48hr before harvest. Immediately prior to collection, 1.25μM Calcein-AM (final concentration)(SantaCruz, sc-203865) was added to each well and incubated for 15 minutes. The plates were then imaged on a Molecular Devices ImageXpress XL. 21 high magnification fluorescence images were captured for each well (23.9% of total well surface area) using a 10x Objective (Nikon Plan Fluor, 0.3 NA). Cell number was assessed using MetaXpress Software with Powercore using the Multi-wavelength cell scoring module. Following imaging, cells are dissolved in 6M Guanidine HCl and transferred to glass tubes for derivitiziation with 3M methanolic guanidine HCl. Samples were prepared alongside standard curve samples made up of FAMES mix (Nu-chek Prep, GLC 20a) and Cholesterol (Sigma, C8667).

Total cellular fatty acids were prepared by mild acid methanolysis [72] with the following modifications: a total acid methanolysis reaction volume of 720μl was used with .6% HCl (w/v). 0.17μg of trinonadecanoin (Nu-chek Prep, T-165) and Stigmastanol (Sigma, S4297) were added to each reaction as internal standard for FAMES and Cholesterol analysis respectively. Following extraction of resulting FAMES and sterols with 1mL of hexane, 25ul of sample was analyzed for FAMES by GC/MS using an Agilent 7890B/5977A with DB-WAX column (Agilent,

122-7032). Complete GC-MS configurations and running programs available upon request. Sterols contained within remaining sample were derivatized with 5µl of anhydrous pyridine (Sigma, 270970) and 5µl BSTFA + TMCS, 99:1 (Sigma, 33155-U). 25ul of sample was run on Agilent 7890B/5977A with ZB-MR1 column (Zebron 7HG-G016-11).

Integration and quantification of all ions performed on MassHunter Quantitative Analysis Program (Agilent Technologies, B.06.00). Analysis for total quantification of Fatty Acids and Cholesterol and relative contributions of synthesis to the respective pool over labeling period were determined by fitting the isotopologue distributions to Isotopomer Spectral Analysis (ISA) as previously described [16].

Chapter 3: Figure 1

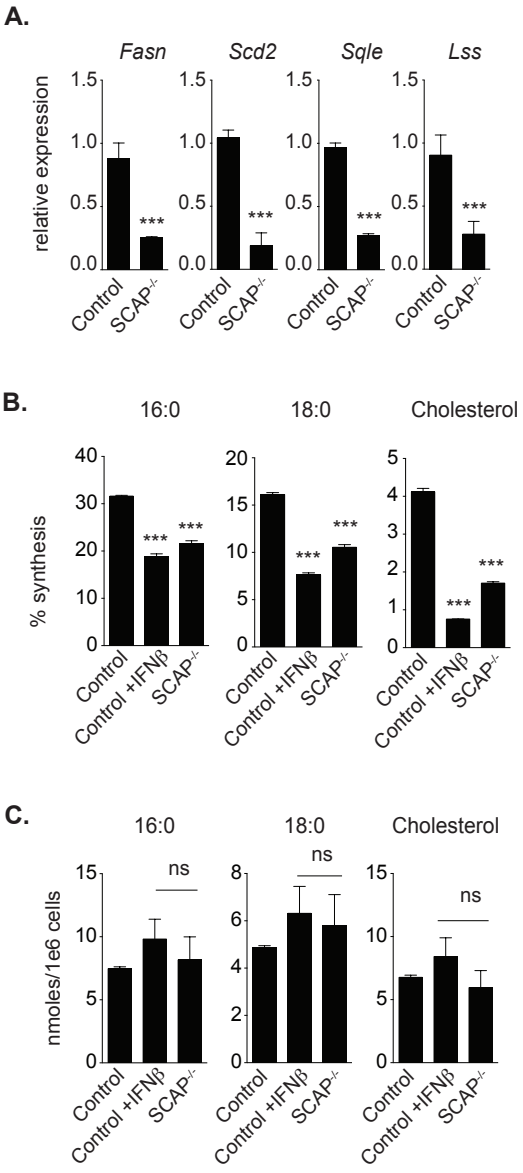

Chapter 3: Figure 1. Genetic deletion of SCAP shifts the balance of lipid synthesis and import in macrophage (A) qPCR analysis of *Fasn*, *Scd2*, *Sqle*, and *Lss* gene expression in quiescent LysM $Cre^{+/-}$ control (designated Control) or LysM $Cre^{+/-}$ $SCAP^{fl/fl}$ ($SCAP^{-/-}$). **(B)** Percent synthesis of palmitic acid (16:0), stearic acid (18:0) and cholesterol as measured by ISA of Control or $SCAP^{-/-}$ BMDMs unstimulated or stimulated with IFNβ as above for 24h. **(C)** Total cellular palmitic acid (16:0), stearic acid (18:0) and cholesterol from Control or $SCAP^{-/-}$ BMDMs unstimulated or stimulated with IFNβ as above for 24h. All mass spec and gene expression experiments are expressed as means ± SD from three independent experiments, unless noted otherwise. $*P < 0.05$; $**P < 0.01$, $***P < 0.005$ (unpaired Student's *t* test).

Chapter 3: Figure 2

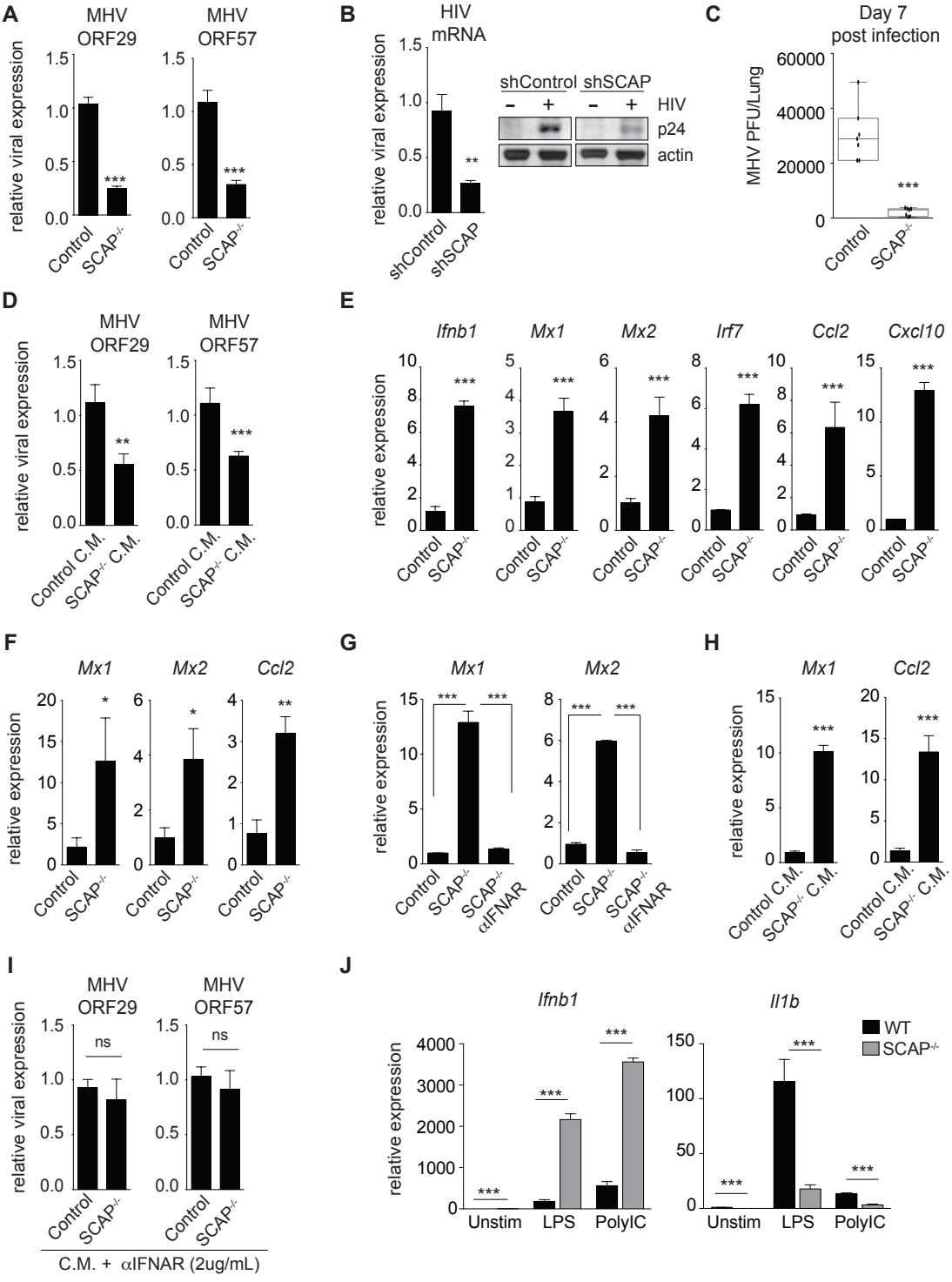

Chapter 3: Figure 2. Genetic inhibition of the lipid biosynthetic program primes antiviral immunity. **(A)** qPCR analysis of murine gammaherpesvirus-68 (MHV-68) genes ORF29 and ORF57 in Control or $SCAP^{-/-}$ BMDMs infected with MHV-68 (MOI=0.5) for 48h. **(B)** qPCR analysis of HIV-1 mRNA (left) and representative immunoblots of HIV-1 p24 protein levels (right) from shControl or shSCAP THP1 macrophages 96h after infection. **(C)** MHV-68 titers from the lungs of LysM $Cre^{+/-}$ control (Control) or LysM $Cre^{+/-}$ $SCAP^{fl/fl}$ ($SCAP^{-/-}$) mice on d.7 post intranasal infection (N=7; data shown is the combined results from two separate infection experiments of n=3 per group and n=4 per group). **(D)** MHV-68 ORF29 and ORF57 gene expression in WT BMDMs pretreated for 4h with Control or $SCAP^{-/-}$ conditioned media (C.M.) before MHV-68 infection (MOI=0.5) for 48h. C.M. from Control or $SCAP^{-/-}$ BMDMs was collected on d.7 post-differentiation. **(E)** qPCR analysis of *Ifnb1* and representative interferon stimulated genes (ISGs) in unstimulated control or $SCAP^{-/-}$ BMDMs on d.7 of differentiation. **(F)** qPCR analysis of ISGs in *ex vivo* alveolar macrophage isolated from bronchoalveolar lavage from LysM $Cre^{+/-}$ control (Control) or LysM $Cre^{+/-}$ $SCAP^{fl/fl}$ ($SCAP^{-/-}$) (3 mice/group). **(G)** qPCR analysis of *Mx1* and *Mx2* in unstimulated control or $SCAP^{-/-}$ BMDMs on d.9 of differentiation +/- 5ug/mL IFNAR blocking antibody for last 48h. **(H)** qPCR analysis of ISGs in WT BMDMs treated for 4h with Control or $SCAP^{-/-}$ conditioned media (C.M.). **(I)** MHV-68 ORF29 and ORF57 gene expression in WT BMDMs pretreated for 4h with Control or $SCAP^{-/-}$ conditioned media (CM) + 2ug/mL IFNAR blocking antibody before MHV-68 infection (MOI=0.5) for 48h. **(J)** qPCR analysis of *Ifnb1* and *Il1b* gene expression in Control or $SCAP^{-/-}$ BMDMs unstimulated or stimulated with LPS (50ng/mL) or Poly:IC (1ug/mL) for 1h on d.8 of differentiation. All experiments are reported as means ± SD from three independent experiments unless noted otherwise. $*P < 0.05$; $**P < 0.01$, $***P < 0.005$ (unpaired Student's *t* test).

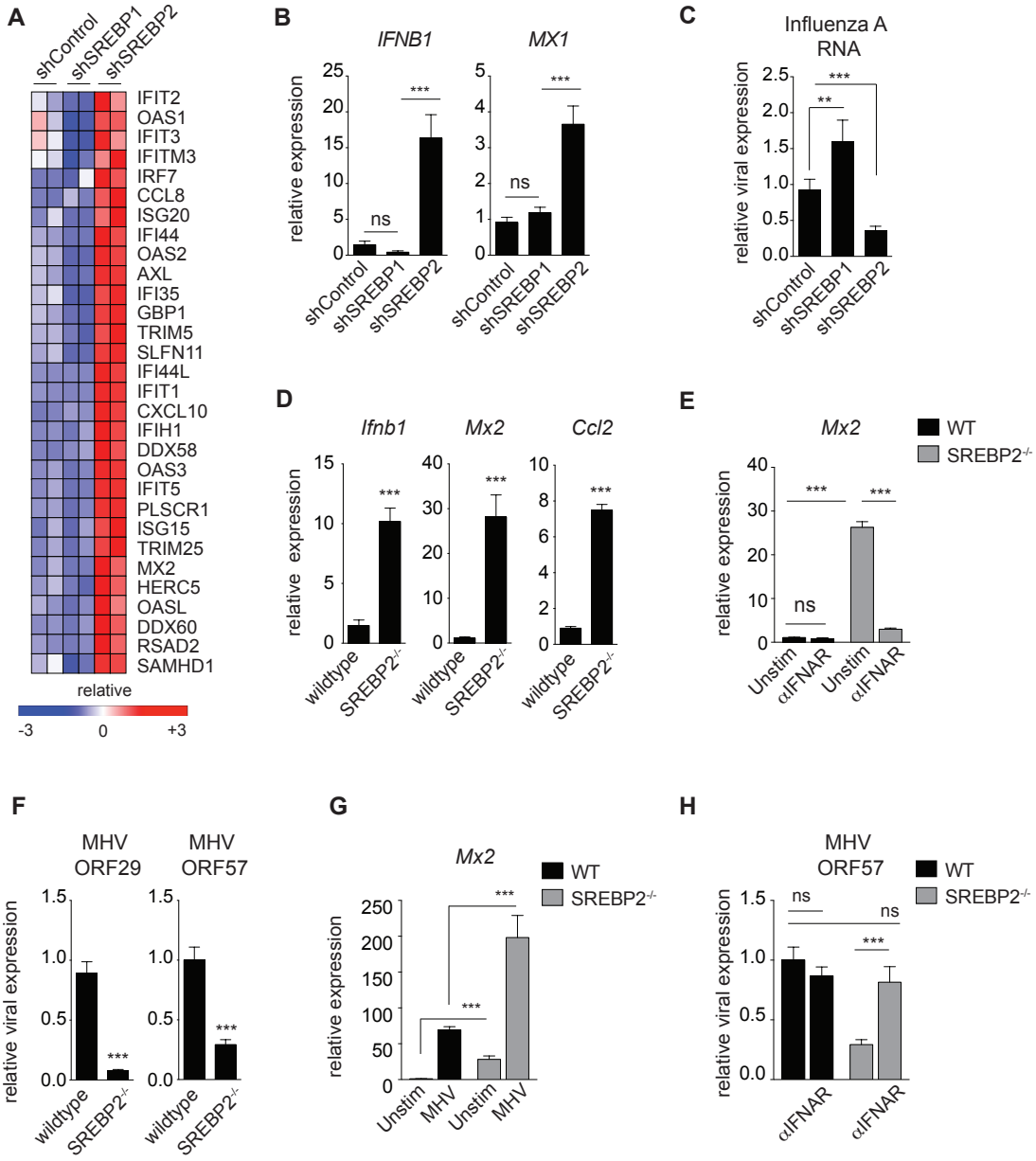
A
shControl
shSREBP1
shSREBP2
IFIT2
OAS1
IFIT3
IFITM3
IRF7
CCL8
ISG20
IFI44
OAS2
AXL
IFI35
GBP1
TRIM5
SLFN11
IFI44L
IFIT1
CXCL10
IFIH1
DDX58
OAS3
IFIT5
PLSCR1
ISG15
TRIM25
MX2
HERC5
OASL
DDX60
RSAD2
SAMHD1
relative
-3
0
+3
B
IFNB1
MX1
relative expression
ns
***
shControl
shSREBP1
shSREBP2
C
Influenza A RNA
relative viral expression
**
***
D
Ifnb1
Mx2
Ccl2
relative expression
wildtype
SREBP2-/-
E
Mx2
WT
SREBP2-/-
relative expression
Unstim
αIFNAR
F
MHV ORF29
MHV ORF57
relative viral expression
G
Mx2
WT
SREBP2-/-
relative expression
Unstim
MHV
H
MHV ORF57
WT
SREBP2-/-
relative viral expression
ns
αIFNAR

Chapter 3: Figure 3. Inhibiting the SREBP2 transcriptional pathway engages a type I IFN inflammatory response. (A) RNA-seq data from unstimulated shControl, shSREBP1 and shSREBP2 THP1 cells 72 h after PMA-differentiation into macrophages. Data shown are biologic replicates of each genotype. **(B)** qPCR analysis of *IFNB1* and *MX1* genes in unstimulated shControl, shSREBP1 and shSREBP2 primary PBMC-derived human macrophages. **(C)** qPCR analysis of Influenza A RNA from shControl, shSREBP1 or shSREBP2 THP1 cells 72h post infection. **(D)** qPCR analysis of *Ifnb1, Mx2* and *Ccl2* gene expression in WT control or SREBP2$^{-/-}$ mouse embryonic fibroblasts (MEFs) cultured in DMEM containing 1% FBS for 24h. **(E)** qPCR analysis of *Mx2* gene expression in WT or SREBP2$^{-/-}$ MEFs cultured in 1% FBS for 24h +/- 5ug/mL IFNAR blocking antibody as indicated **(F)** qPCR analysis of MHV-68 ORF29 and ORF57 gene expression in WT or SREBP2$^{-/-}$ MEFs infected with MHV-68 (MOI=1.0) for 24h . **(G)** qPCR analysis of *Mx2* in WT or SREBP2$^{-/-}$ MEFs +/- MHV infection (MOI=1.0) for 24h. **(H)** qPCR analysis of MHV-68 ORF57 gene expression in WT or SREBP2$^{-/-}$ MEFs infected with MHV-68 (MOI=1.0) for 24h +/- 24h pretreatment with 5ug/mL IFNAR blocking antibody. All experiments are reported as means ± SD from three independent experiments. *P < 0.05; **P < 0.01, ***P < 0.005 (unpaired Student's t test).

Chapter 3: Figure 4

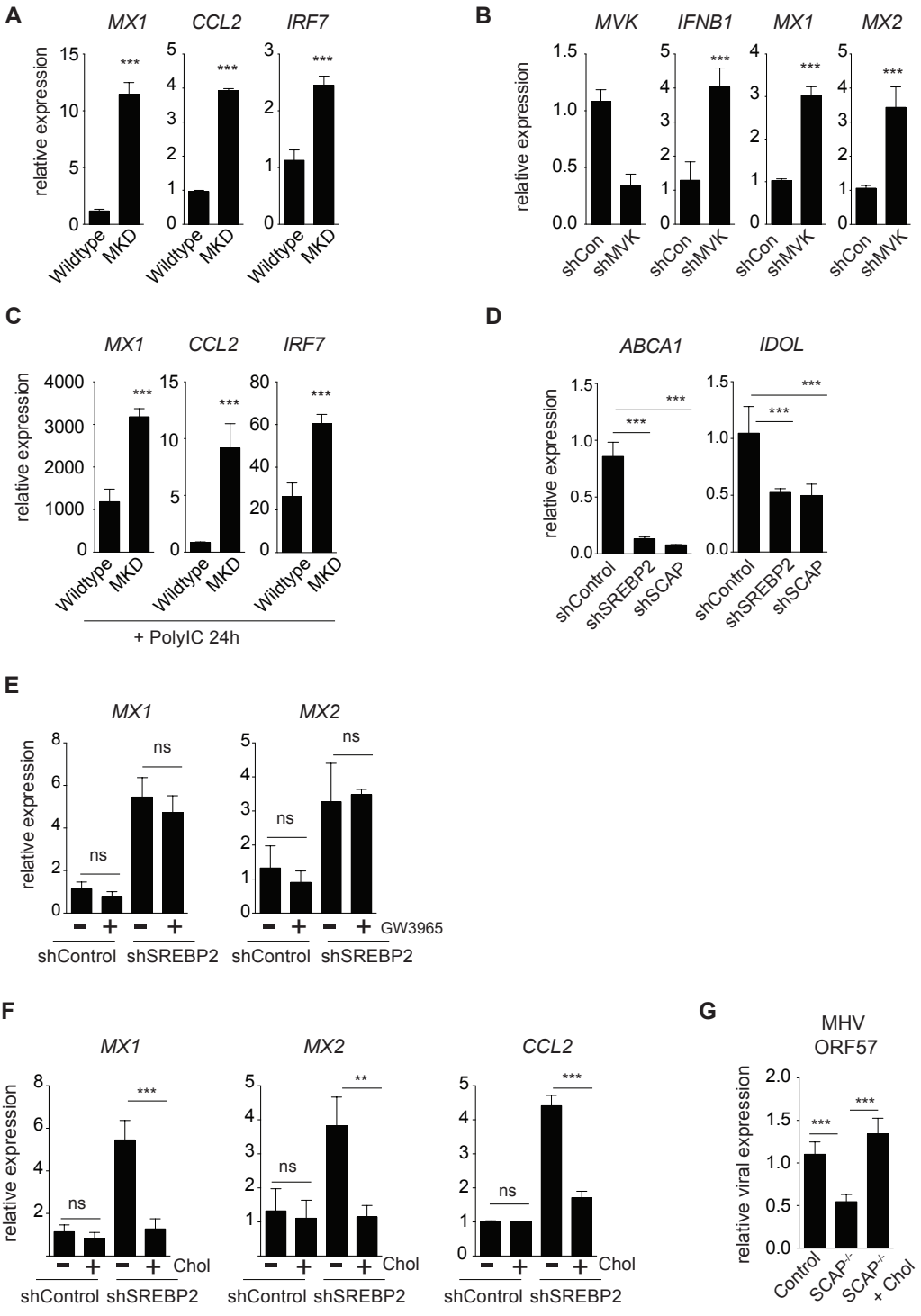

Chapter 3: Figure 4: Limiting flux throught the cholesterol biosynthetic pathway engages a type I IFN response. (A) qPCR analysis of ISG expression in population control (Wildtype) primary human fibroblasts or fibroblasts from an individual with MVK-deficiency (MKD; ~2% MVK activity compared to population controls). **(B)** qPCR analysis of *MVK, IFNB1* and ISG expression in shControl or shMVK THP1 cells after 72h of PMA-differentiation **(C)** qPCR analysis of ISG expression in population control (Wildtype) primary human fibroblasts or fibroblasts from an individual with MVK-deficiency (MKD) primed with 2ug/mL Poly:IC for 24h. **(D)** qPCR analysis of *ABCA1* and *IDOL* gene expression in shControl, shSREBP2 and shSCAP THP1 macrophages differentiated for 72h. **(E)** qPCR analysis of *MX1* and *MX2* gene expression in THP1 shControl or shSREBP2 cells differentiated as above and stimulated with vehicle (DMSO) or LXR ligand (1uM GW3965) for 72h. **(F)** qPCR analysis of *MX1, MX2* and *CCL2* gene expression of differentiated THP1 shControl or shSREBP2 macrophages in media supplemented with 0.1mg/mL methyl beta cyclodextrin (MβCD)-cholesterol (labeled as "Chol") as indicated for 72h. **G.** qPCR analysis of MHV-68 ORF57 gene expression in Control or $SCAP^{-/-}$ BMDMs +/- 0.25mg/mL MβCD-cholesterol (Chol) for 48h, then infected with MHV-68 (MOI=0.5) for 24h. All experiments are reported as means ± SD from three independent experiments. $*P < 0.05$; $**P < 0.01$, $***P < 0.005$ (unpaired Student's *t* test).

Chapter 3: Figure 5

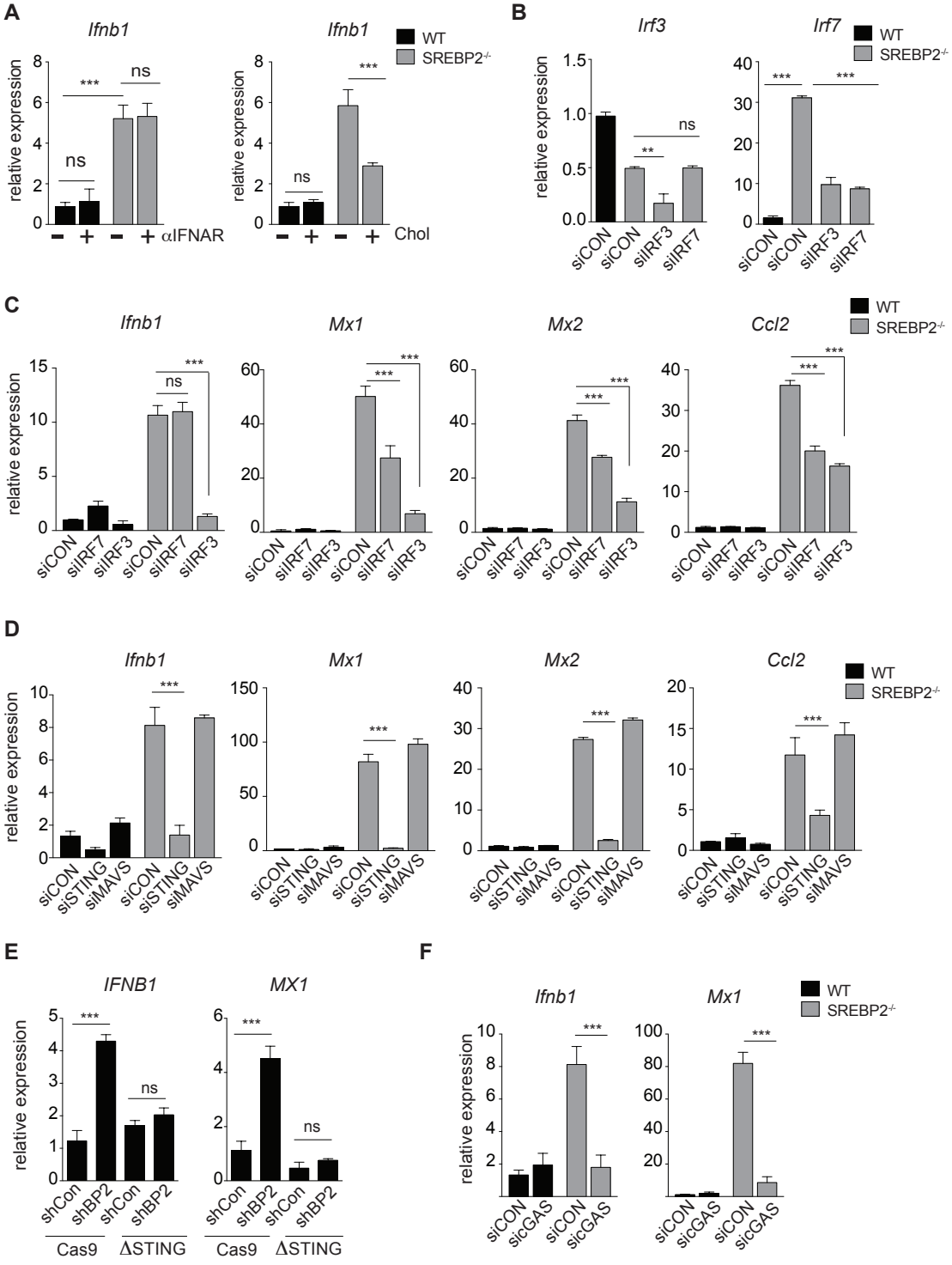

Chapter 3: Figure 5. IRF3/STING link changes in cholesterol biosynthesis with type I IFN production. (A) Left: qPCR analysis of *Ifnb1* gene expression in WT or SREBP2$^{-/-}$ MEFs cultured in 1% FBS for 24h +/- 5ug/mL IFNAR blocking antibody as indicated. Right: qPCR analysis of *Ifnb1* gene expression in WT and SREBP2$^{-/-}$ MEFs treated 0.075mg/mL MβCD-cholesterol (Chol) as indicated for 72h. **(B)** qPCR analysis of *Irf3* and *Irf7* in WT or SREBP2$^{-/-}$ MEFs transfected with control siRNA, siIRF3 or siIRF7 **(C)** qPCR analysis of *Ifnb1, Mx1, Mx2* and *Ccl2* in WT or SREBP2$^{-/-}$ MEFs transfected with control siRNA, siIRF3 or siIRF7 **(D)** qPCR analysis of *Ifnb1, Mx1, Mx2* and *Ccl2 in* WT or SREBP2$^{-/-}$ MEFs transfected with control siRNA, siMAVS or siSTING as indicated **(E)** qPCR of *IFNB1* and *MX1* gene expression from control (Cas9) or CRISPR/Cas9-edited STING (ΔSTING) THP1 cells stably transduced with shControl or shSREBP2. **(F)** qPCR analysis of *Ifnb1* and *Mx1* in WT or SREBP2$^{-/-}$ MEFs transfected with control siRNA or siRNA to cGAS. All experiments are reported as means ± SD from three independent experiments. **P* < 0.05; ***P* < 0.01, ****P* < 0.005 (unpaired Student's *t* test).

Chapter 3: Figure 6

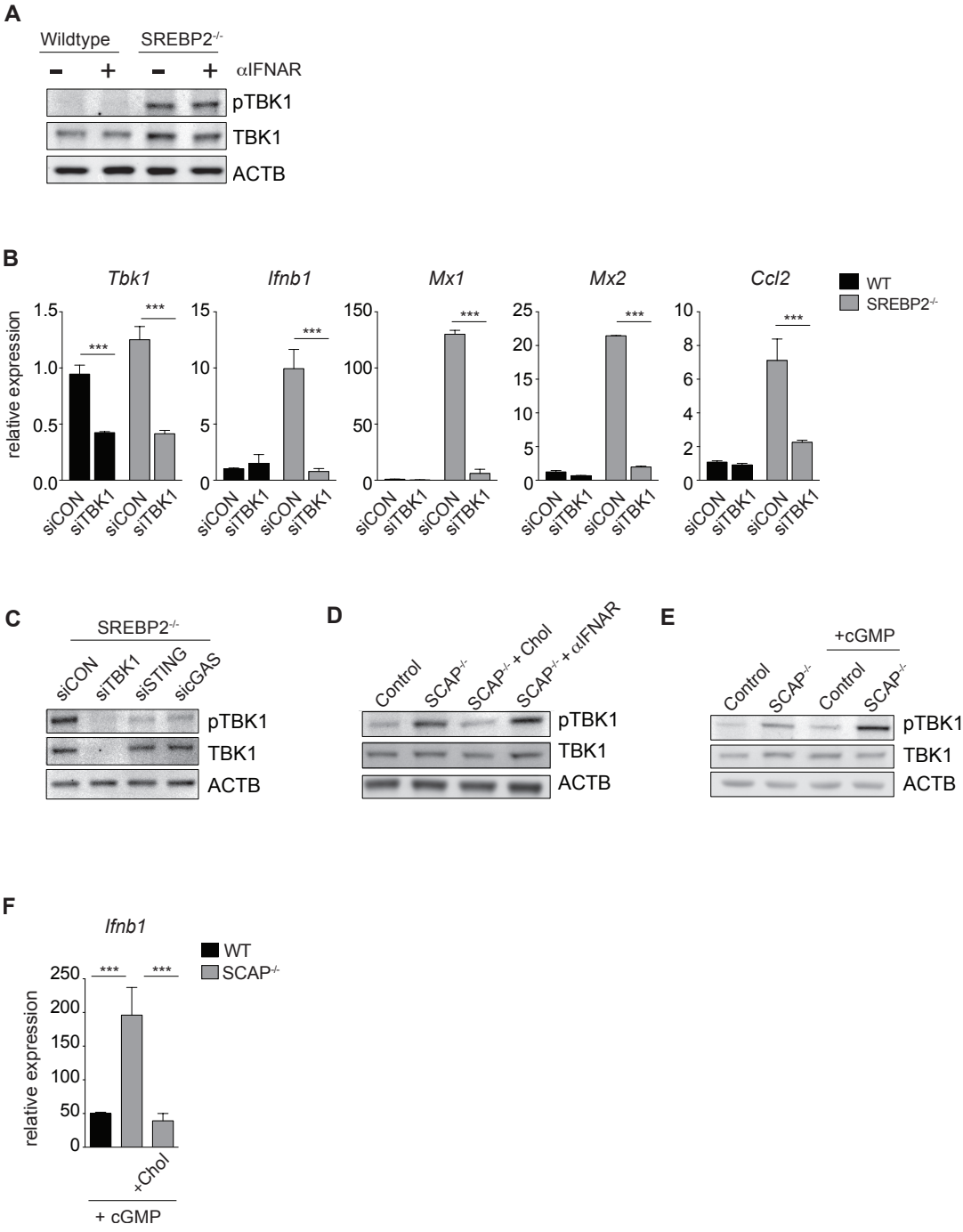

Chapter 3: Figure 6: Perturbations in cholesterol homeostasis alters STING sensitivity to di-cyclic nucleotides. (A) Western blot analysis of phospho-TBK1 (pTBK1) and total TBK1 from whole cell lysates in WT or SREBP2$^{-/-}$ MEFs cultured in 1% FBS for 24h +/- 5ug/mL IFNAR blocking antibody as indicated. **(B)** qPCR analysis of *Tbk1, Ifnb1, Mx1, Mx2* and *Ccl2 in* WT or SREBP2$^{-/-}$ MEFs transfected with control siRNA, or siTBK1. **(C)** Western blot analysis of phospho-TBK1 (pTBK1) and total TBK1 from whole cell lysates of SREBP2$^{-/-}$ MEFs transfected with control siRNA, siSTING or sicGAS as indicated. **(D)** Western blot analysis of phospho-TBK1 (pTBK1) and TBK1 total in Control or SCAP$^{-/-}$ BMDMs +/- 0.25mg/mL MβCD-cholesterol (Chol) for 48h or 10ug/mL IFNAR neutralizing antibody. **(E)** Western blot analysis of phospho-TBK1 (pTBK1) and TBK1 total in Control or SCAP$^{-/-}$ BMDMs +/- 5ug/mL c-di-GMP (cGMP) for 45 min. **(F)** qPCR analysis of *Ifnb1* gene expression in Control or SCAP$^{-/-}$ BMDMs. BMDMs were cultured +/- 0.25mg/mL MβCD-cholesterol for 48h, then stimulated with 5ug/mL c-di-GMP (cGMP) for 1h.

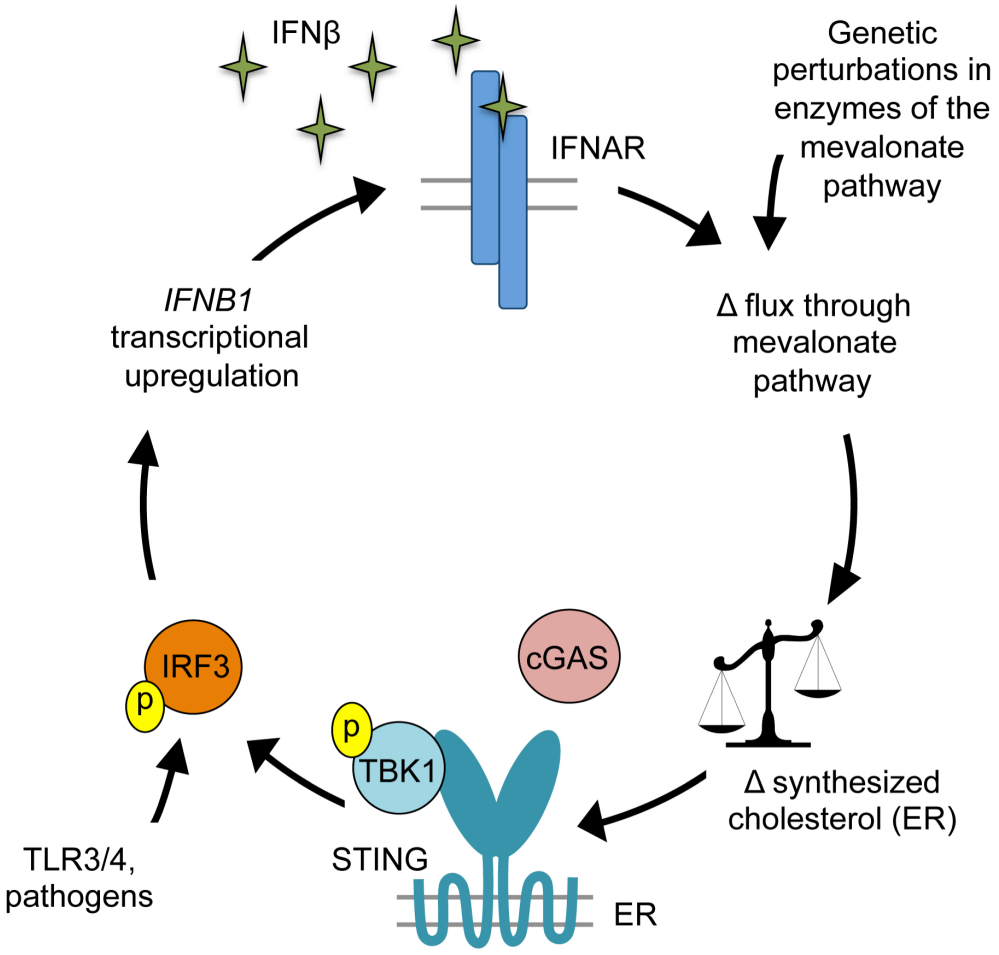

Chapter 3: Figure 7: A metabolic-inflammatory circuit. Type I IFN signaling limits biosynthetic flux through the mevalonate pathway. Repression of the mevalonate pathway lowers cholesterol synthesis resulting in STING activation, TBK1 phosphorylation and subsequent IRF3-mediated production of type I IFN. In this system, the mevalonate pathway and IFN-signaling pathway are part of a metabolic-inflammatory circuit that ensures any changes in the activity of one pathway are sensed by the other pathway.

Chapter 3: Supplemental Figure 1

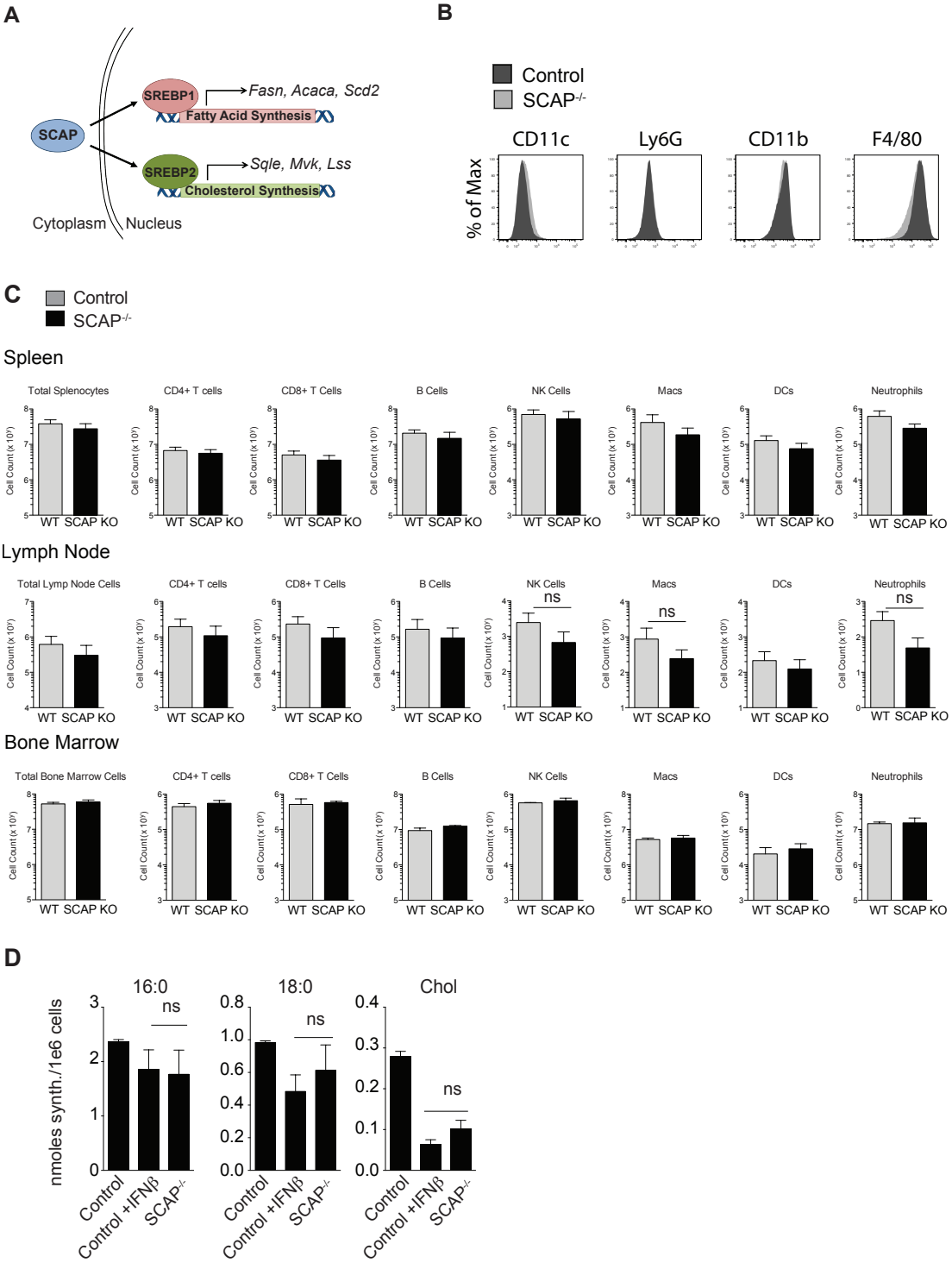

Chapter 3: Supplemental Figure 1. Genetic deletion of SCAP in macrophage phenocopies type I IFN mediated alterations in lipid metabolism. (A) Schematic: SREBP cleavage activating protein (SCAP) regulates the activity of sterol regulatory element proteins SREBP1 and 2. Deletion of SCAP attenuates both SREBP1 and 2, resulting in decreased expression of fatty acid and cholesterol synthesis genes. **(B)** Flow cytometry analysis of CD11c, Ly6G, CD11b and F4/80 staining from LysM Cre+ Control or LysM Cre+ $SCAP^{-/-}$ BMDM on day 7 post harvest. **(C)** Flow cytometry analysis of the frequency and absolute numbers of macrophage, T cells, B cells, NK cells, dendritic cells, and neutrophil populations in the spleen, bone marrow or lymph nodes of LysM Cre+ Control or LysM Cre+ $SCAP^{-/-}$ mice. **(D)** Net synthesis of palmitic acid (16:0), stearic acid (18:0) and cholesterol as measured by ISA of Control or $SCAP^{-/-}$ BMDMs unstimulated or stimulated with IFNβ as above for 24h.

Chapter 3: Supplemental Figure 2

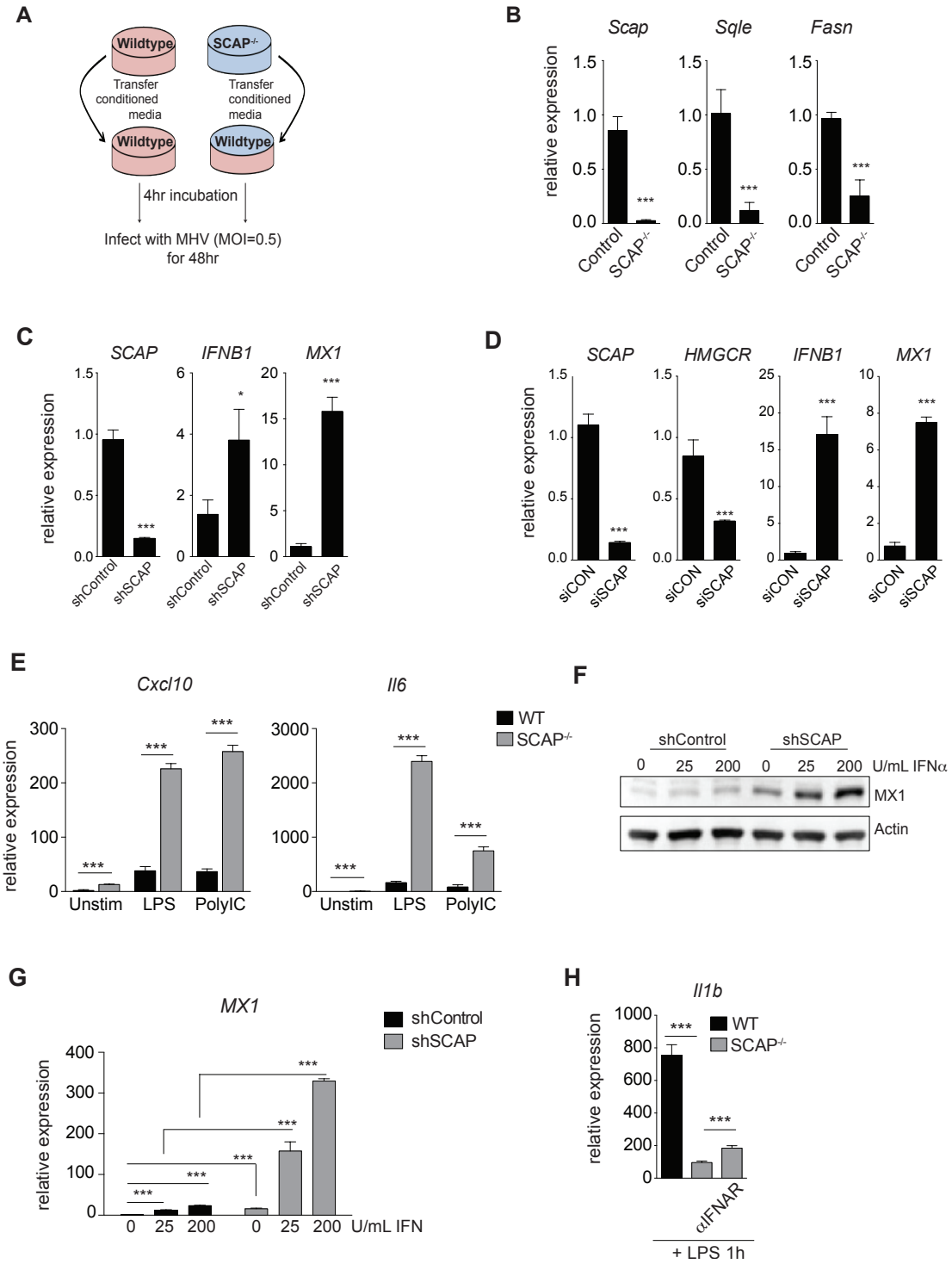

Chapter 3: Supplemental Figure 2. Genetic inhibition of the lipid biosynthetic program primes type I IFN mediated inflammation. (A) Schematic of conditioned media transfer experiment. **(B)** qPCR analysis of lipid biosynthesis genes in *ex vivo* alveolar macrophage from LysM $Cre^{+/-}$ Control (Control) or LysM $Cre^{+/-}$ $SCAP^{fl/fl}$ ($SCAP^{-/-}$) (3 mice/group). **(C)** qPCR analysis of *SCAP, IFNB1* and *MX1* gene expression in unstimulated shControl and shSCAP THP1 cells after 72h PMA-differentiation. **(D)** qPCR analysis of *SCAP, HMGCR, IFNB1* and *MX1* gene expression in THP1 cells transfected with siCon (non-targeting scramble siRNA) or siSCAP. **(E)** qPCR analysis of *Cxcl10* and *Il6* gene expression in Control or $SCAP^{-/-}$ BMDMs unstimulated or stimulated with LPS (50ng/mL) or Poly:IC (1ug/mL) for 1h. **(F)** Representative western blots of MX1 in shControl and shSCAP THP1 cells plus 4h treatment with IFNα as indicated. **(G)** qPCR analysis of *MX1* gene expression in shControl and shSCAP THP1 cells plus 4h treatment with IFNα as indicated. **(H)** qPCR analysis of *Il1b* gene expression in Control or $SCAP^{-/-}$ BMDMs +/- 10ug/mL IFNAR neutralizing antibody for 24h, then stimulated with LPS (50ng/mL) for 1h. All experiments are reported as means ± SD from three independent experiments. $*P < 0.05$; $**P < 0.01$, $***P < 0.005$ (unpaired Student's *t* test)

Chapter 3: Supplemental Figure 3

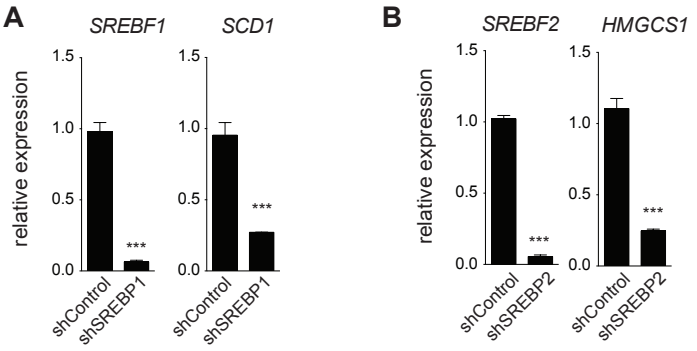

C

Ontology Term	# genes enriched	Adj. enrichment p-value
Immune effector process	33	1.68E-16
innate immune response	33	6.05E-12
immune system process	57	5.72E-14
response to type I interferon	16	2.68E-15
response to virus	33	7.66E-24
defense response to virus	28	1.79E-22
negative reg. of viral reproduction	7	1.00E-06
response to cytokine stimulus	27	1.43E-10
regulation of cytokine production	15	2.00E-04
double-stranded RNA binding	8	1.02E-06
single-stranded RNA binding	5	2.60E-03
response to other organism	39	8.18E-18
response to biotic stimulus	39	5.83E-12

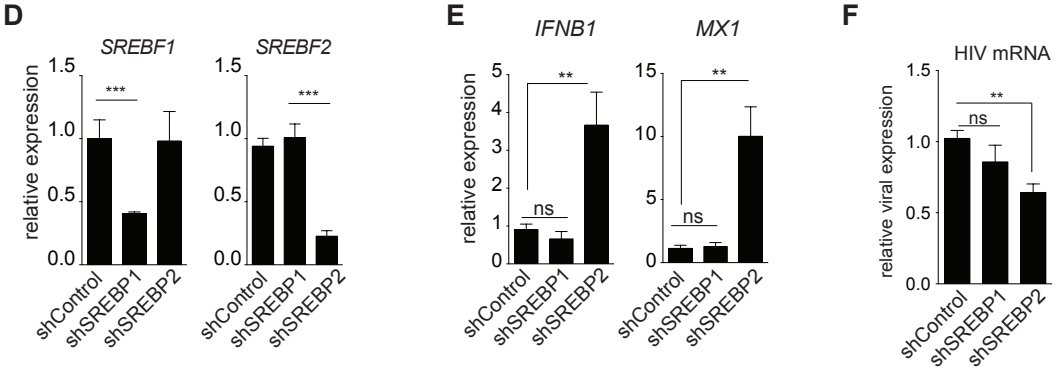

Chapter 3: Supplemental Figure 3. Inhibiting SREBP2 transcriptional pathway engages type I IFN-mediated inflammation. (A) qPCR analysis of *SREBF1* and *SCD1* expression in shControl and shSREBP1 THP1 cells. **(B)** qPCR analysis of *SREBF2* and *HMGCS1* expression in shControl and shSREBP2 THP1 cells. **(C)** Ontology analysis of RNA-Seq data from unstimulated shControl and shSREBP2 THP1 cells 72h after PMA-differentiation into macrophages. Number of genes (# genes) indicates the number of genes enriched in each Ontology Term. Adj. enrichment provides the adjusted p-values to indicate significant enrichment in response to loss of SREBP2 transcriptional responses. **(D)** qPCR analysis of *SREBF1* and *SREBF2* expression in shControl, shSREBP1 and shSREBP2 primary PBMC-derived human macrophages. **(E)** qPCR analysis of *IFNB1* and *MX1* genes in unstimulated shControl, shSREBP1 and shSREBP2 THP1 macrophages 72h after PMA-differentiation. **(F)** qPCR analysis of HIV-1 mRNA from shControl, shSREBP1 or shSREBP2 THP1 macrophages infected for 96h. All experiments reported as means ± SD from three independent experiments. **P* < 0.05; ***P* < 0.01, ****P* < 0.005 (unpaired Student's *t* test)

Chapter 3: Supplemental Figure 4

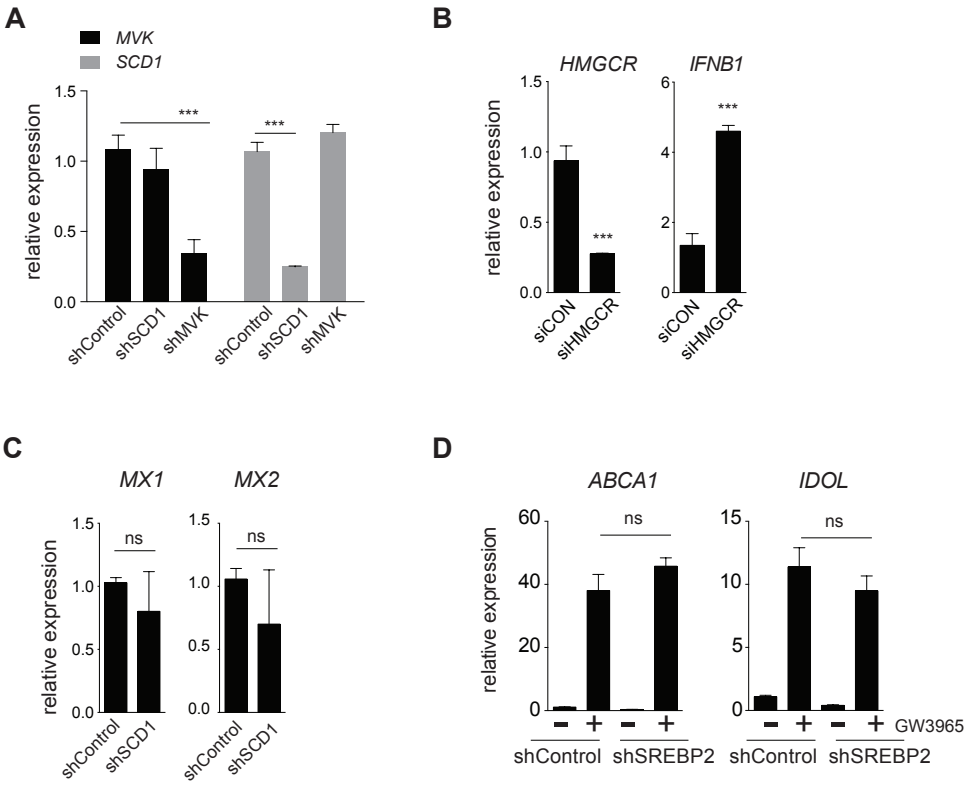

Chapter 3: Supplemental Figure 4. Limiting flux through the mevalonate pathway upregulates type I IFN. (A) qPCR analysis of *MVK* and *SCD1* expression in shControl, shSCD1 and shMVK THP1 cells differentiated for 72h. **(B)** qPCR analysis of *HMGCR* and *IFNB1* expression in THP1 transfected with siCon (non-targeting scramble siRNA) or siHMGCR. **(C)** qPCR analysis of *MX1* and *MX2* expression in shControl and shSCD1 THP1 cells differentiated for 72h. **(D)** qPCR analysis of *ABCA1* and *IDOL* gene expression in THP1 shControl or shSREBP2 cells differentiated as above and stimulated with vehicle (DMSO) or LXR ligand (1uM GW3965) for 72h. All experiments reported as means ± SD from three independent experiments. **P* < 0.05; ***P* < 0.01, ****P* < 0.005 (unpaired Student's *t* test)

Chapter 3: Supplemental Figure 5

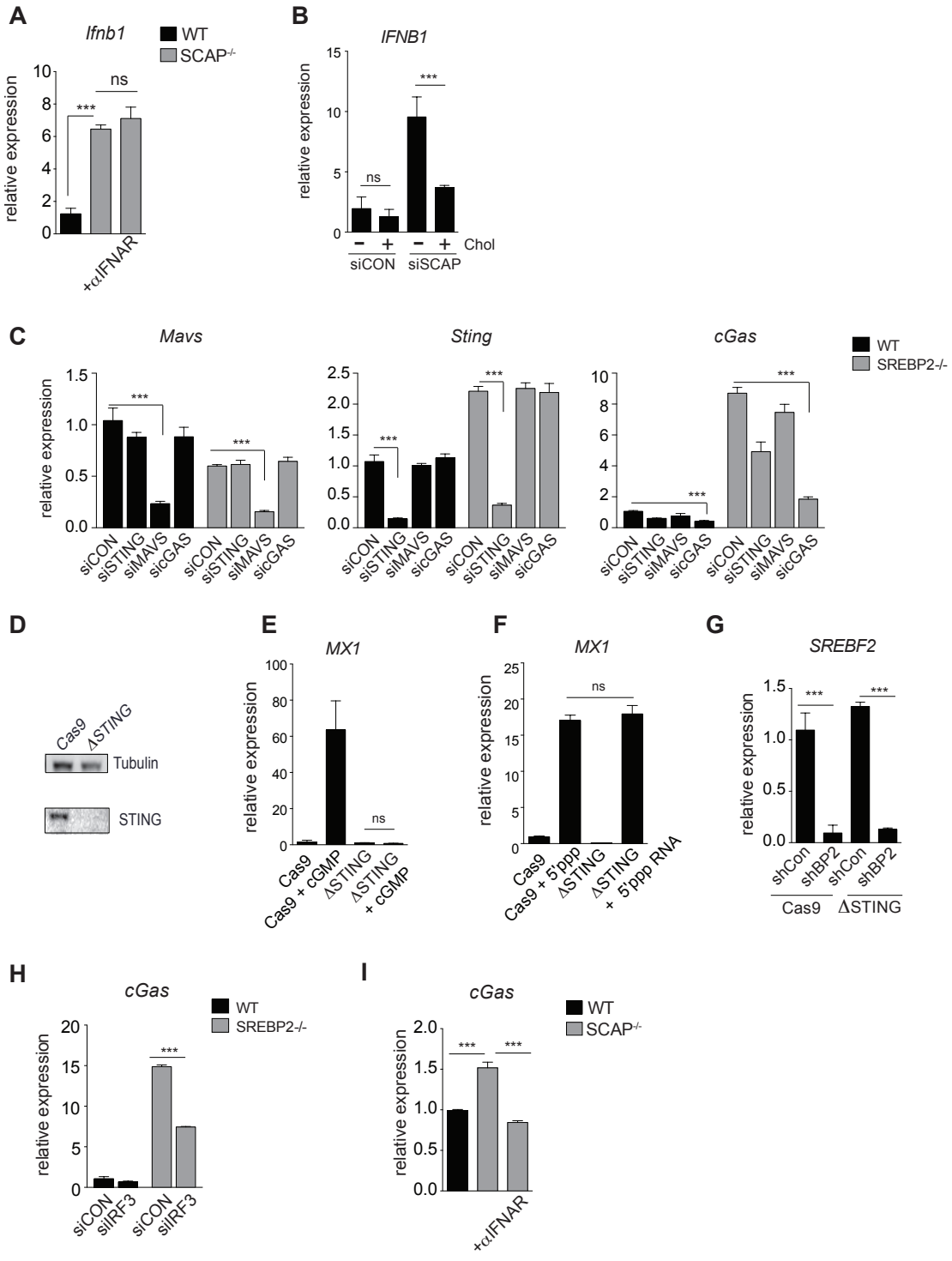

Chapter 3: Supplemental Figure 5. cGAS/STING links type I IFN with changes in cholesterol biosynthetic flux (A) qPCR analysis of *Ifnb1* in unstimulated control or $SCAP^{-/-}$ BMDMs on d.9 of differentiation +/- 5ug/mL IFNAR blocking antibody for last 48h**. (B)** qPCR analysis of *IFNB1* expression THP1 cells transfected with non-targeting scramble siRNA (siCON) or siSCAP. 24h post transfection, cells were changed into fresh media with or without 0.1mg/mL MβCD-cholesterol for an additional 48h. **(C)** qPCR analysis of *Mavs, Sting* and *cGas* expression in WT or SREBP2-null MEFs transfected with siRNAs targeting MAVS, STING or cGAS. **(D)** Representative western blot of STING or tubulin from whole cell lysates from Cas9 control or ΔSTING THP1 cells. **(E & F)** qPCR analysis of *MX1* expression in Cas9 or ΔSTING THP1 cells treated with **(E)** 20uM cyclic-di-GMP (cGMP) for 24h **(F)** 50uM 5'ppp RNA for 12h. **(G)** qPCR of *SREBF2* gene expression from control (Cas9) or CRISPR/Cas9-edited STING (ΔSTING) THP1 cells stably transduced with shControl or shSREBP2. **(H)** qPCR analysis of *cGAS* in WT or $SREBP2^{-/-}$ MEFs transfected with control siRNA, siIRF3 or siIRF7. **(I)** qPCR analysis of *cGas* in unstimulated control or $SCAP^{-/-}$ BMDMs on d.9 of differentiation +/- 5ug/mL IFNAR blocking antibody for last 48h. All experiments are represented as means ± SD from three independent experiments). $*P < 0.05$; $**P < 0.01$, $***P < 0.005$ (unpaired Student's *t* test)

References for Chapter 3:

7. Glass CK, Witztum JL (2001) Atherosclerosis. the road ahead. Cell 104: 503-516.

9. Shibata N, Glass CK (2009) Regulation of macrophage function in inflammation and atherosclerosis. J Lipid Res 50 Suppl: S277-281.

12. Wang ML, Motamed M, Infante RE, Abi-Mosleh L, Kwon HJ, et al. (2010) Identification of surface residues on Niemann-Pick C2 essential for hydrophobic handoff of cholesterol to NPC1 in lysosomes. Cell Metab 12: 166-173.

13. Radhakrishnan A, Goldstein JL, McDonald JG, Brown MS (2008) Switch-like control of SREBP-2 transport triggered by small changes in ER cholesterol: a delicate balance. Cell Metab 8: 512-521.

15. Das A, Brown MS, Anderson DD, Goldstein JL, Radhakrishnan A (2014) Three pools of plasma membrane cholesterol and their relation to cholesterol homeostasis. Elife 3.

16. Williams KJ, Argus JP, Zhu Y, Wilks MQ, Marbois BN, et al. (2013) An essential requirement for the SCAP/SREBP signaling axis to protect cancer cells from lipotoxicity. Cancer Res 73: 2850-2862.

17. Kidani Y, Elsaesser H, Hock MB, Vergnes L, Williams KJ, et al. (2013) Sterol regulatory element-binding proteins are essential for the metabolic programming of effector T cells and adaptive immunity. Nat Immunol 14: 489-499.

19. Horton JD, Goldstein JL, Brown MS (2002) SREBPs: activators of the complete program of cholesterol and fatty acid synthesis in the liver. J Clin Invest 109: 1125-1131.

22. Spann NJ, Garmire LX, McDonald JG, Myers DS, Milne SB, et al. (2012) Regulated accumulation of desmosterol integrates macrophage lipid metabolism and inflammatory responses. Cell 151: 138-152.

23. Yang C, McDonald JG, Patel A, Zhang Y, Umetani M, et al. (2006) Sterol intermediates from cholesterol biosynthetic pathway as liver X receptor ligands. J Biol Chem 281: 27816-27826.

49. Parihar SP, Guler R, Khutlang R, Lang DM, Hurdayal R, et al. (2014) Statin therapy reduces the mycobacterium tuberculosis burden in human macrophages and in mice by enhancing autophagy and phagosome maturation. J Infect Dis 209: 754-763.

50. Rzouq F, Alahdab F, Olyaee M (2014) Statins and hepatitis C virus infection: an old therapy with new scope. Am J Med Sci 348: 426-430.

51. Gilbert C, Bergeron M, Methot S, Giguere JF, Tremblay MJ (2005) Statins could be used to control replication of some viruses, including HIV-1. Viral Immunol 18: 474-489.

52. Blanc M, Hsieh WY, Robertson KA, Watterson S, Shui G, et al. (2011) Host defense against viral infection involves interferon mediated down-regulation of sterol biosynthesis. PLoS Biol 9: e1000598.

55. Reboldi A, Dang EV, McDonald JG, Liang G, Russell DW, et al. (2014) Inflammation. 25-Hydroxycholesterol suppresses interleukin-1-driven inflammation downstream of type I interferon. Science 345: 679-684.

72. Ichihara K, Fukubayashi Y (2010) Preparation of fatty acid methyl esters for gas-liquid chromatography. J Lipid Res 51: 635-640.

73. Hughes DJ, Kipar A, Sample JT, Stewart JP (2010) Pathogenesis of a model gammaherpesvirus in a natural host. J Virol 84: 3949-3961.

74. Esposito S, Ascolese B, Senatore L, Bosis S, Verrecchia E, et al. (2014) Current advances in the understanding and treatment of mevalonate kinase deficiency. Int J Immunopathol Pharmacol 27: 491-498.

75. Santos JA, Arostegui JI, Brito MJ, Neves C, Conde M (2014) Hyper-IgD and periodic fever syndrome: a new MVK mutation (p.R277G) associated with a severe phenotype. Gene 542: 217-220.

76. Castrillo A, Joseph SB, Vaidya SA, Haberland M, Fogelman AM, et al. (2003) Crosstalk between LXR and toll-like receptor signaling mediates bacterial and viral antagonism of cholesterol metabolism. Mol Cell 12: 805-816.

77. Honda K, Yanai H, Negishi H, Asagiri M, Sato M, et al. (2005) IRF-7 is the master regulator of type-I interferon-dependent immune responses. Nature 434: 772-777.

78. Fitzgerald KA, McWhirter SM, Faia KL, Rowe DC, Latz E, et al. (2003) IKKepsilon and TBK1 are essential components of the IRF3 signaling pathway. Nat Immunol 4: 491-496.

79. Ishikawa H, Barber GN (2008) STING is an endoplasmic reticulum adaptor that facilitates innate immune signalling. Nature 455: 674-678.

80. Tanaka Y, Chen ZJ (2012) STING specifies IRF3 phosphorylation by TBK1 in the cytosolic DNA signaling pathway. Sci Signal 5: ra20.

81. Sun L, Wu J, Du F, Chen X, Chen ZJ (2013) Cyclic GMP-AMP synthase is a cytosolic DNA sensor that activates the type I interferon pathway. Science 339: 786-791.

82. Seth RB, Sun L, Ea CK, Chen ZJ (2005) Identification and characterization of MAVS, a mitochondrial antiviral signaling protein that activates NF-kappaB and IRF 3. Cell 122: 669-682.

83. Chow OA, von Kockritz-Blickwede M, Bright AT, Hensler ME, Zinkernagel AS, et al. (2010) Statins enhance formation of phagocyte extracellular traps. Cell Host Microbe 8: 445-454.

84. Guarda G, Braun M, Staehli F, Tardivel A, Mattmann C, et al. (2011) Type I interferon inhibits interleukin-1 production and inflammasome activation. Immunity 34: 213-223.

85. Sun LP, Seemann J, Goldstein JL, Brown MS (2007) Sterol-regulated transport of SREBPs from endoplasmic reticulum to Golgi: Insig renders sorting signal in Scap inaccessible to COPII proteins. Proc Natl Acad Sci U S A 104: 6519-6526.

86. West AP, Khoury-Hanold W, Staron M, Tal MC, Pineda CM, et al. (2015) Mitochondrial DNA stress primes the antiviral innate immune response. Nature.

87. White MJ, McArthur K, Metcalf D, Lane RM, Cambier JC, et al. (2014) Apoptotic caspases suppress mtDNA-induced STING-mediated type I IFN production. Cell 159: 1549-1562.

88. Neumann G, Watanabe T, Ito H, Watanabe S, Goto H, et al. (1999) Generation of influenza A viruses entirely from cloned cDNAs. Proc Natl Acad Sci U S A 96: 9345-9350.

89. Eckard SC, Rice GI, Fabre A, Badens C, Gray EE, et al. (2014) The SKIV2L RNA exosome limits activation of the RIG-I-like receptors. Nat Immunol 15: 839-845.

90. Dobin A, Davis CA, Schlesinger F, Drenkow J, Zaleski C, et al. (2013) STAR: ultrafast universal RNA-seq aligner. Bioinformatics 29: 15-21.

91. Anders S, Pyl PT, Huber W (2015) HTSeq-a Python framework to work with high-throughput sequencing data. Bioinformatics 31: 166-169.

92. Anders S, Huber W (2010) Differential expression analysis for sequence count data. Genome Biol 11: R106.

93. Si Y, Liu P, Li P, Brutnell TP (2014) Model-based clustering for RNA-seq data. Bioinformatics 30: 197-205.

94. Wang J, Duncan D, Shi Z, Zhang B (2013) WEB-based GEne SeT AnaLysis Toolkit (WebGestalt): update 2013. Nucleic Acids Res 41: W77-83.